Scuola di Dottorato Leonardo da Vinci – a.a. 2012/13

LASER: CARATTERISTICHE, PRINCIPI FISICI, APPLICAZIONI

Versione 4 – July 13 – http://www.df.unipi.it/~fuso/dida

Part 7
Diode lasers:
technology and a few applications

OUTLOOK

- Short hystory of diode lasers and of their (huge) impact on the market:
  - technological progress (from 60's to now)
  - groundbreaking applications

- Diode and junctions:
  - semiconductors and semiconductive alloys
  - homojunction laser (not working…)
  - heterojunctions, heterostructures, MQWs and excitons
  - technology and related issues (also for the future)

- Quantum Cascade Lasers (QCLs):
  - fabrication
  - operation and applications

Objective : to see how microelectronics has given a big impulse onto laser technology and to review applicative pros and cons of diode lasers

LASER MARKET ISSUES

Rough estimation of the cost for a laser device (order of magnitude):
- Laser Ar^+ for metrology or optical pump in laser systems: tens of kE
- Laser CO_2 for industrial applications: hundred kE
- Excimer laser for lithography, optical marking, material treatment: hundreds kE
- Laser Nd:YAG for industrial applications: tens/hundred kE
- Laser Ti:Sa with femtosecond pulses (pumps included): hundreds kE

- Diode lasers: a few Euros (up to thousands of Euros for high end systems)!!!

Diode lasers fully exploit the advancements in microelectronics, including VLSI, to offer to the market devices for market-oriented applications (consumer)

For instance, blue diode lasers reduced their cost by roughly two orders of magnitude in the last 10-15 years, corresponding to the explosion of the optical data storage market (presently not so vital, yet!)

Similarly, QCLs are now commercially available for sensing applications with a cost markedly reduced with respect to their introduction

HYSTORICAL NOTE

The first semiconductor lasers were realized in 1962 almost simultaneously by research groups from General Electric (GE) Laboratories, IBM Research Division, and Massachusetts Institute of Technology (MIT) Lincoln Laboratories. These early devices operated only at cryogenic temperatures or under pulsed conditions. They were homojunction lasers, which means that the same material (GaAs) was used in the active region as well as for the p- and n-doped side of the laser diode junction. In 1963, Herbert Kroemer from the University of Colorado came up with the idea of heterostructure lasers, where a thin active layer is sandwiched between two slabs of different material having a higher band-gap energy to confine the carriers, but it lasted until 1970 before this idea was realized in the AlGaAs/GaAs material system, leading to the first semiconductor lasers that operated continuously at room temperature. In the following two decades, there was a dramatic development in the device properties and an extension of the emission-wavelength range that was mainly driven by the development of fiber communication systems.

Zhores I. Alferov

The Nobel Prize in Physics 2000

Nobel Lecture

Double Heterostructure Concept and its Applications in Physics, Electronics and Technology

Zhores I. Alferov held his Nobel Lecture December 8, 2000, at Aula Magna, Stockholm University. He was presented by Professor Stig Hagström.

A nice case story: diode lasers have invaded the market in the last two decades

But

ideas are much older and time was needed for technolgy to evolve (e.g., MBE)

(Note: evolution of the technology has been driven by applications!)

(MAYBE) IN THE FUTURE LASERS WILL BE MADE OF "PLASTICS"??

Photonic Frontiers: Organic Semiconductor Lasers - The pump is the challenge

Light-emitting organic semiconductors fall into two broad categories: small molecules and conjugated polymers. Both types are used in OLED fabrication, but laser developers have focused on conjugated polymers, which can be deposited from solution or printed by ink-jet-like devices.

Organic semiconductors have important attractions that extend beyond the ability to fabricate them in inexpensive arrays for OLED displays. In polymers, the semiconducting properties arise from overlap in electron orbits along carbon chains where single and double bonds alternate. Both emission and absorption bands are inherently wide, and wavelength ranges can be chosen by selecting the compounds that make up the polymer. Like laser dyes, both emission bands and absorption bands are broad, allowing both wavelength tuning and short-pulse generation. The absorption bands are strong and widely separated from fluorescence bands, as required for high gain.

Although electrical excitation seems easy for organic LEDs, several issues combine to make it a particularly tough problem for organic semiconductor lasers. One is lower electron mobility than in inorganic semiconductors, which limits current flow in organic materials. Although OLEDs can be driven with a current density of just 0.01 A/cm^2, organic semiconductors can't withstand the current densities of 1000 A/cm^2 needed to drive an inorganic diode laser. To make matters worse, lasers are far more vulnerable to cavity losses than LEDs, and organic diodes suffer losses from electrical contacts and the depletion of excitons by junction current. "The more charge you throw into the cavity, the more excitons get annihilated, so your quantum efficiency gets worse as you pump it harder," says Stephen Forrest of the University of Michigan (Ann Arbor, MI).

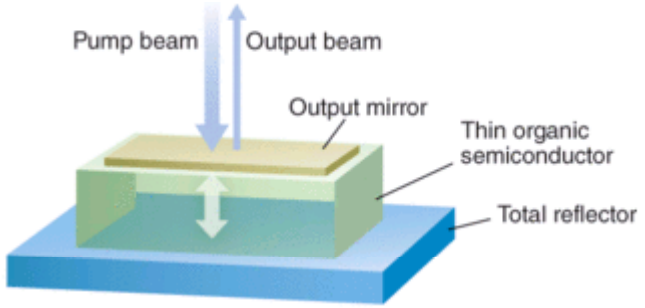

FIGURE 1. Optical pumping of a polymer thin film sandwiched in a Fabry-Perot cavity shows that gain can be high, but power is low because the cavity is very thin.

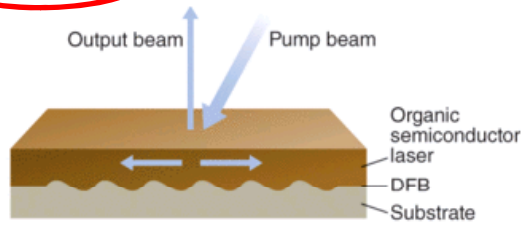

FIGURE 3. A distributed-feedback grating on the substrate scatters light both vertically, to produce the output beam, and horizontally, so the beam can be amplified in the plane of the organic semiconductor layer.

Some key technical issues remain to be overcome, such as improving operating lifetimes of the organic laser materials. But the big question about organic semiconductor lasers is which way the field will go—toward perfecting optically pumped versions or toward a new approach to electrical pumping.

Samuel says that optically pumping with an LED is a key advance toward practical devices. "If you have a low-cost package that gives you a versatile laser that has wires hanging off that you connect to a battery, no one will really care that the charges are injected into the nitride and the light comes from the polymer," he explains. The average user doesn't care if a green-laser pointer is diode-pumped doubled neodymium or direct-diode laser emission, and optical pumping is much easier to achieve. "I'm hopeful that in five years time, rather than wondering when they finally will get injection lasers, I hope they forget why they wanted injection lasers," he says.

A few years ago, people were actively dreaming of organic lasers (cheap, flexible, biocompatible, etc.)
Now, I don't know…

LARGE SCALE APPLICATIONS (A FEW WORDS) I

One big and still growing application field for diode lasers is optical TLC

Optical fiber is used by many telecommunications companies to transmit telephone signals, Internet communication, and cable television signals. Due to much lower attenuation and interference, optical fiber has large advantages over existing copper wire in long-distance and high-demand applications. However, infrastructure development within cities was relatively difficult and time-consuming, and fiber-optic systems were complex and expensive to install and operate. Due to these difficulties, fiber-optic communication systems have primarily been installed in long-distance applications, where they can be used to their full transmission capacity, offsetting the increased cost. Since 2000, the prices for fiber-optic communications have dropped considerably. The price for rolling out fiber to the home has currently become more cost-effective than that of rolling out a copper based network. Prices have dropped to $850 per subscriber[*citation needed*] in the US and lower in countries like The Netherlands, where digging costs are low.

Since 1990, when optical-amplification systems became commercially available, the telecommunications industry has laid a vast network of intercity and transoceanic fiber communication lines. By 2002, an intercontinental network of 250,000 km of submarine communications cable with a capacity of 2.56 Tb/s was completed, and although specific network capacities are privileged information, telecommunications investment reports indicate that network capacity has increased dramatically since 2004.

Advantages:

- Immune to e.m. noise
- Inherently long haul
- Less expensive (due to the fiber cost with respect to copper)
- Fast and huge bandwidth (especially with wavelength division multiplexing – WDM)

Main requirements on laser sources:

- Miniaturized and easily coupled to fibers
- Wavelengths in the TLC windows
- Pulsed (with seamless, e.g., electronics operation)

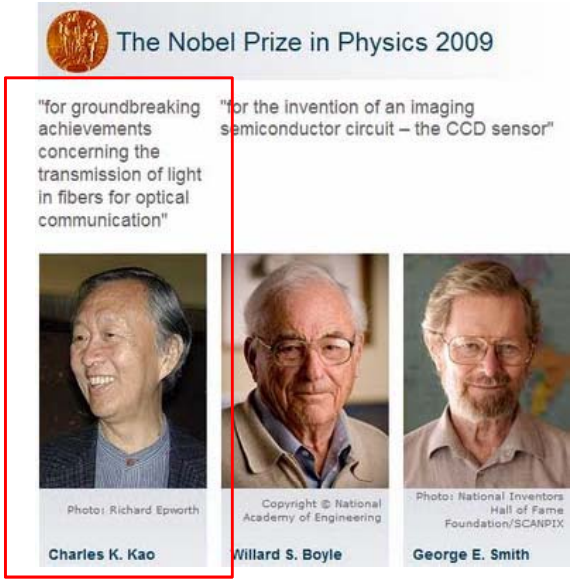

OPTICAL FIBERS AND TLC

Roughly:
the core has a lower refractive index than the cladding
--> ***total internal reflection*** *(lossless) occurs at the core/cladding interface*

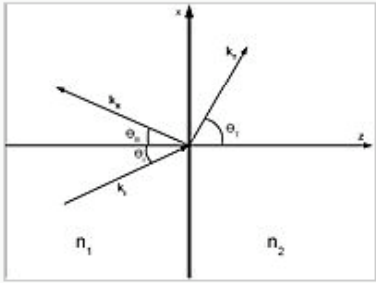

Illustration of Snell's law,
$n_1 \sin\theta_i = n_2 \sin\theta_t$.

The critical angle is the angle of incidence *above* which total internal reflection occurs. The angle of incidence is measured with respect to the normal at the refractive boundary (see diagram illustrating Snell's law). Consider a light ray passing from glass into air. The light emanating from the interface is bent towards the glass. When the incident angle is increased sufficiently, the transmitted angle (in air) reaches 90 degrees. It is at this point no light is transmitted into air. The critical angle θ_c is given by Snell's law,

$$n_1 \sin\theta_i = n_2 \sin\theta_t.$$

Rearranging Snell's Law, we get incidence

$$\sin\theta_i = \frac{n_2}{n_1}\sin\theta_t.$$

To find the critical angle, we find the value for θ_i when θ_t =90° and thus $\sin\theta_t = 1$. The resulting value of θ_i is equal to the critical angle θ_c.

Now, we can solve for θ_i, and we get the equation for the critical angle:

$$\theta_c = \theta_i = \arcsin\left(\frac{n_2}{n_1}\right),$$

If the incident ray is precisely at the critical angle, the refracted ray is tangent to the boundary at the point of incidence. If for example, visible light were traveling through acrylic glass (with an index of refraction of approximately 1.50) into air (with an index of refraction of 1.00), the calculation would give the critical angle for light from acrylic into air, which is

$$\theta_c = \arcsin\left(\frac{1.00}{1.50}\right) = 41.8°.$$

Light incident on the border with an angle less than 41.8° would be partially transmitted, while light incident on the border at larger angles with respect to normal would be totally internally reflected.

ATTENUATION AND "WINDOWS"

Glass optical fibers are almost always made from silica, but some other materials, such as fluorozirconate, fluoroaluminate, and chalcogenide glasses as well as crystalline materials like sapphire, are used for longer-wavelength infrared or other specialized applications. Silica and fluoride glasses usually have refractive indices of about 1.5, but some materials such as the chalcogenides can have indices as high as 3. Typically the index difference between core and cladding is less than one percent.

Fiber attenuation, which necessitates the use of amplification systems, is caused by a combination of material absorption, Rayleigh scattering, Mie scattering, and connection losses. Although material absorption for pure silica is only around 0.03 dB/km (modern fiber has attenuation around 0.3 dB/km), impurities in the original optical fibers caused attenuation of about 1000 dB/km. Other forms of attenuation are caused by physical stresses to the fiber, microscopic fluctuations in density, and imperfect splicing techniques.

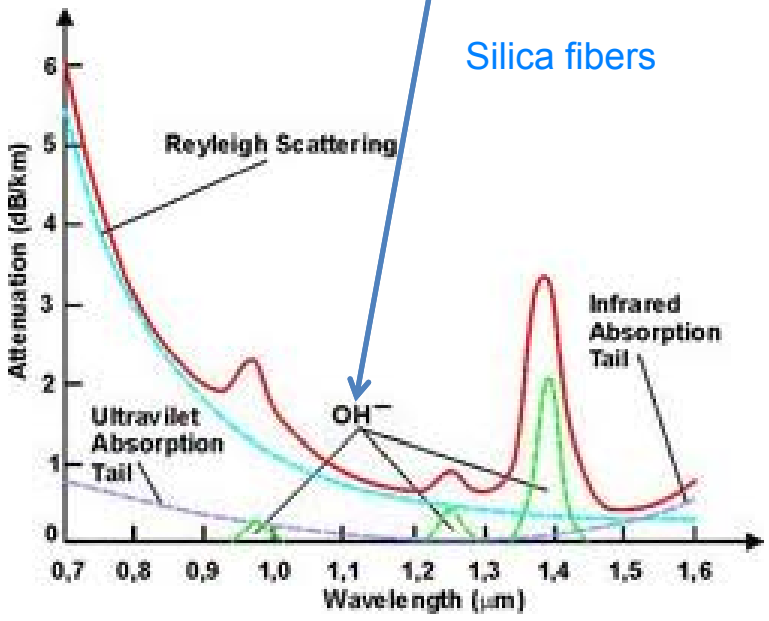

Band	Description	Wavelength Range
O band	original	1260 to 1360 nm
E band	extended	1360 to 1460 nm
S band	short wavelengths	1460 to 1530 nm
C band	conventional ("erbium window")	1530 to 1565 nm
L band	long wavelengths	1565 to 1625 nm
U band	ultralong wavelengths	1625 to 1675 nm

Er+-doped fibers can amplify through Amplifed Stimulated Emission (ASE)
Similar to laser, but this is truly an amplifier rather than an oscillator!

Sources (lasers) must operate in the infrared range

DEMULTIPLEXING AND SPEED

In fiber-optic communications, **wavelength-division multiplexing** (**WDM**) is a technology which multiplexes a number of optical carrier signals onto a single optical fiber by using different wavelengths (i.e. colors) of laser light. This technique enables bidirectional communications over one strand of fiber, as well as multiplication of capacity.

Pulses at different wavelengths are sent into the same fiber (and then demultiplexed by, e.g, a prism)

Different carriers share the same fiber cord enhancing the TLC bandwidth

Year	Organization	Effective speed	WDM channels	Per channel speed	Distance
2009	Alcatel-Lucent[7]	15 Tbit/s	155	100 Gbit/s	90 km
2010	NTT[8]	69.1 Tbit/s	432	171 Gbit/s	240 km
2011	KIT[9]	26 Tbit/s	1	26 Tbit/s	50 km
2011	NEC[10]	101 Tbit/s	370	273 Gbit/s	165 km
2012	NEC, Corning[11]	1.05 Petabit/s	12 core fiber		52.4 km

Monochromaticity is a stringent requirement

Furthermore, efficient coupling with the fiber is desired (lasers are better than other sources, e.g., LEDs)

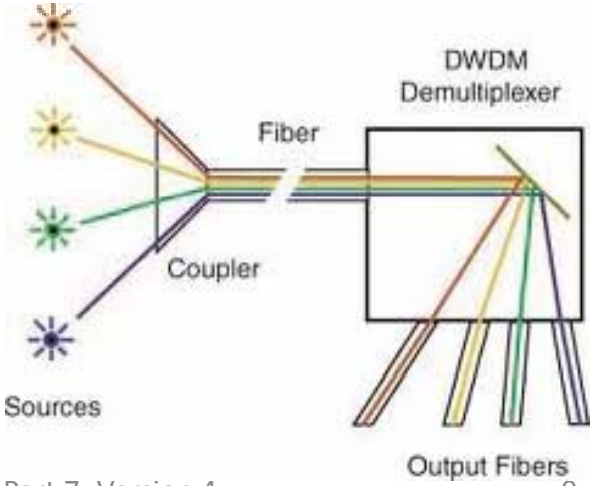

LARGE SCALE APPLICATIONS (A FEW WORDS) II

Optical data storage has been another relevant application (still now, but not so urgent)

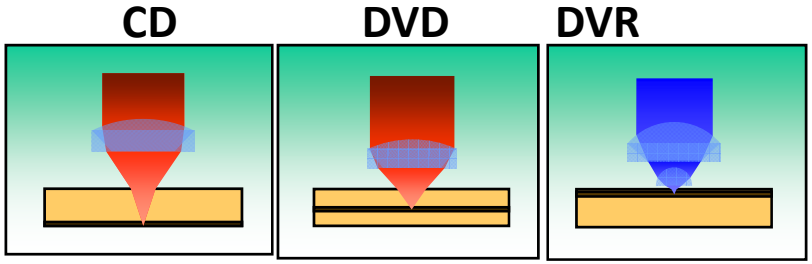

λ (nm)	780	650	400
NA	0.45	0.6	0.85
Capacity (GB)	0.65	4.7	22

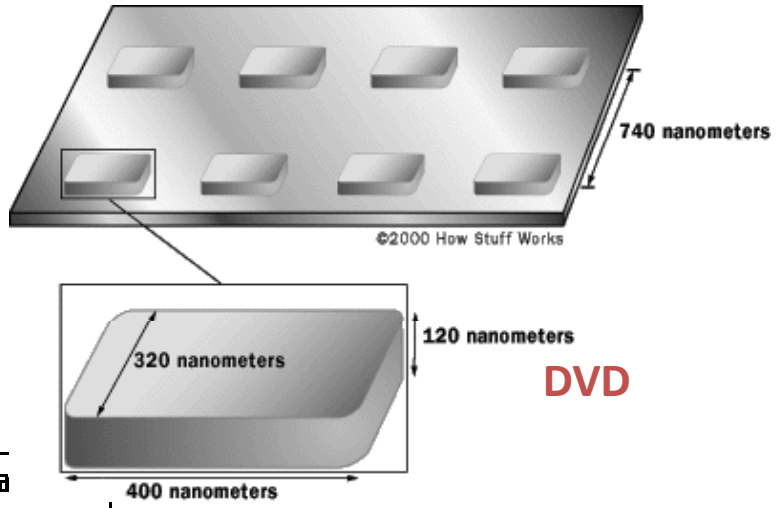

Parameter	CD	DVD	4th Genera
λ (nm)	780	650	400
NA	0.45	0.60	0.85-1.5
Track pitch (μm)	1.6	0.74	0.3-0.15
Velocity (m s-1)	1.2	4.0	3-25
Substrate thickness (mm)	1.2	0.6	1.2-2
Spot size λ/2NA (μm)	0.9	0.55	0.25-0.13
Capacity (GB)	0.65	4.7	100

Laser spot minimum size is affected by diffraction

⇩

Optics with larger NA (we will see!) and lasers with shorter wavelength must be used to increase the storage density

Note: the table refers to the situation in 2005…

Coherent light (M-number close to 1) strictly needed to achieve tight focusing!

ULTRA-HIGH DENSITY DATA STORAGE?

Main requirements on laser sources:

- Coherent
- Emission in the blue/UV
- Portable and cheap

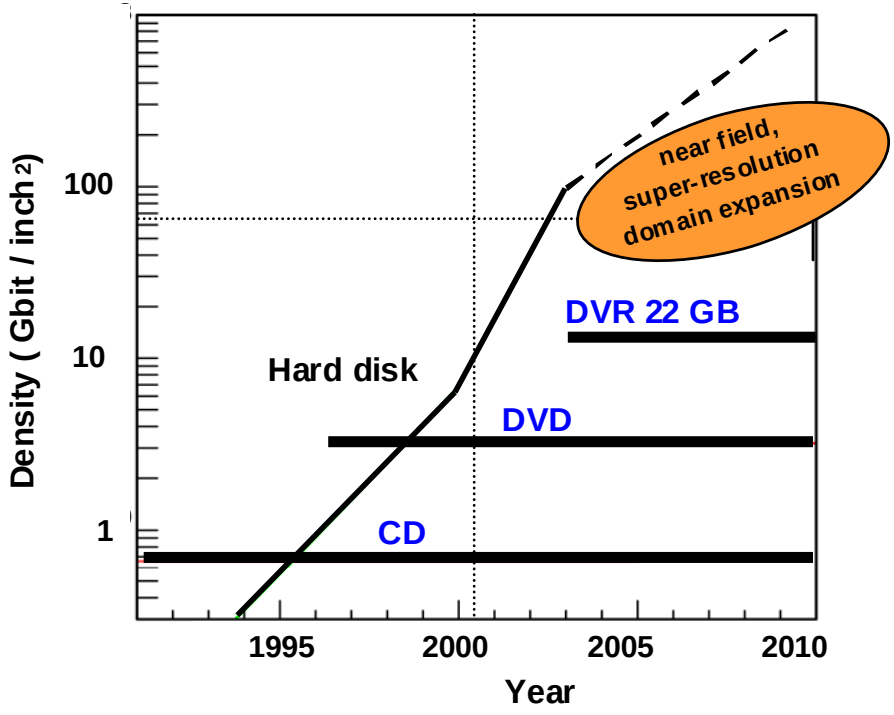

Example of an attempt to optically writing at the nanoscale (with a **near-field** microscope using polarized laser light at 473 nm)

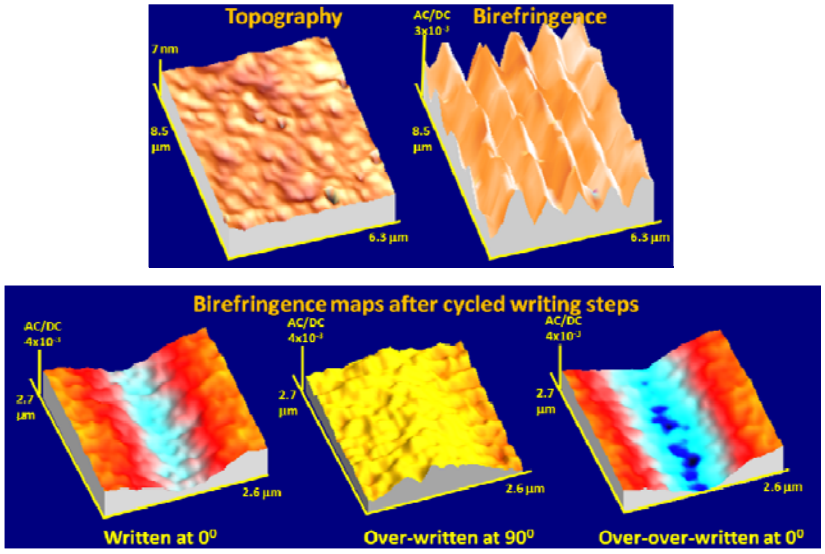

Material: azobenzene containing polymer

Near-field optical writing shows limitations due to the material homogeneity rather than the writing method

REMINDERS ON ENERGY BANDS IN SOLIDS

For a single atom, energy levels are discrete

For a molecule, i.e., a system of *few* bound atoms, levels are splitted into a manifold (splitting is caused by the inter-atom interaction)

When many many atoms are bond together such as in a crystal, the energy splitting into many closely spaced levels gives rise to the occurrence of energy **bands**

The energy of the different bands (and their separation) depend on the material

Filling with electrons of the bands follows specific rules

Materials having "overlapped" bands are conductors, otherwise a band gap appears and materials are semiconductors or dielectrics (depending on the gap width)**:**

Valence and Conduction bands appear

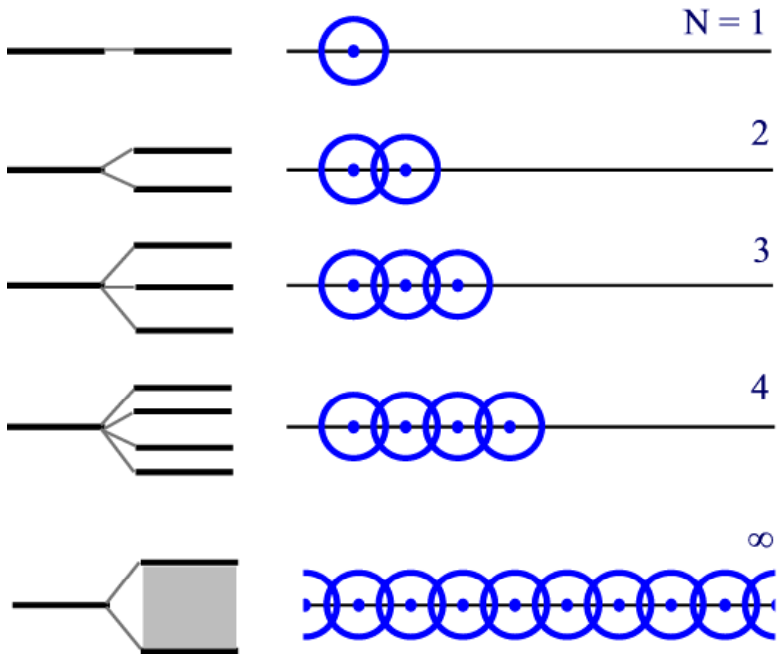

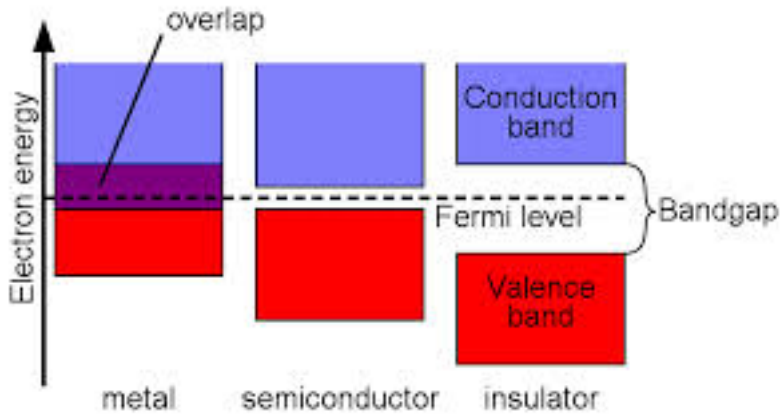

REMINDERS ON p-n JUNCTIONS AND DIODES I

For the moment, let's consider Silicon as the prototypal semiconductive material (it's **not used** in lasers!)
$\Delta E_{gap} \approx$ 1.1-1.2 eV (corresponding to photon energy in the near IR)

Semiconductors can be easily doped with impurities: **donors** provide with a free electron, **acceptors** "eat" a free electron hence provide with a *"hole" (a positive free charge)*

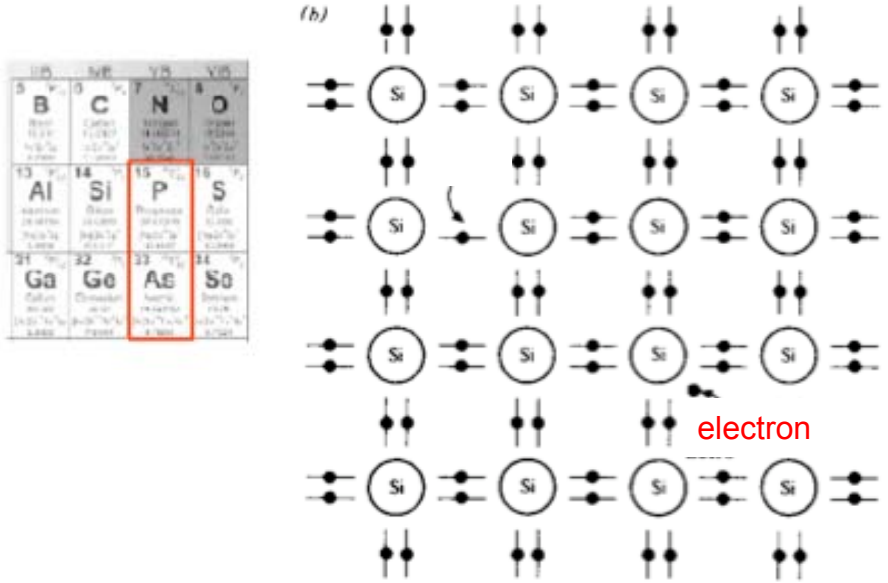

n-doping

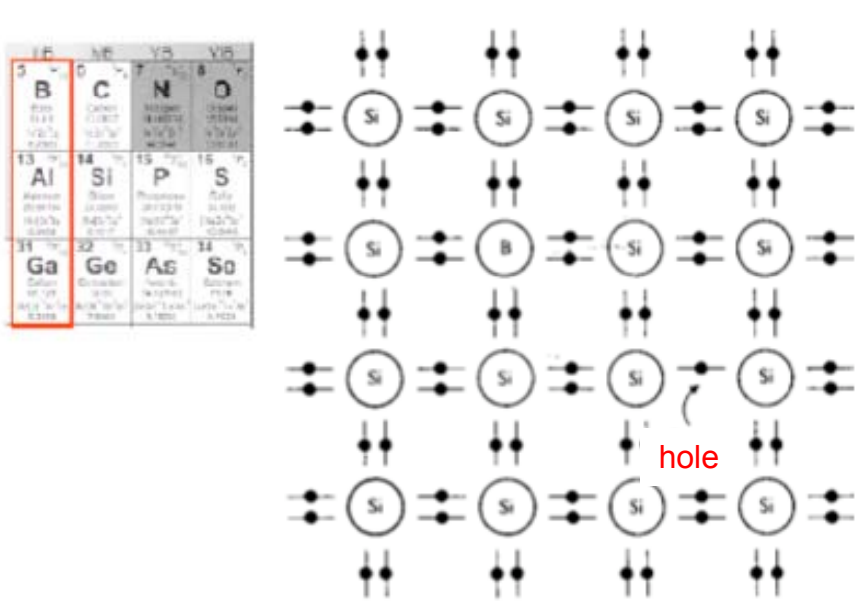

p-doping

By itself, the semiconductor is not a good conductor
The possibility to dope can make it a good/very good conductor **using both negative and positive charge carriers**

REMINDERS ON p-n JUNCTIONS AND DIODES II

No bias applied (unpolarized - equilibrium)

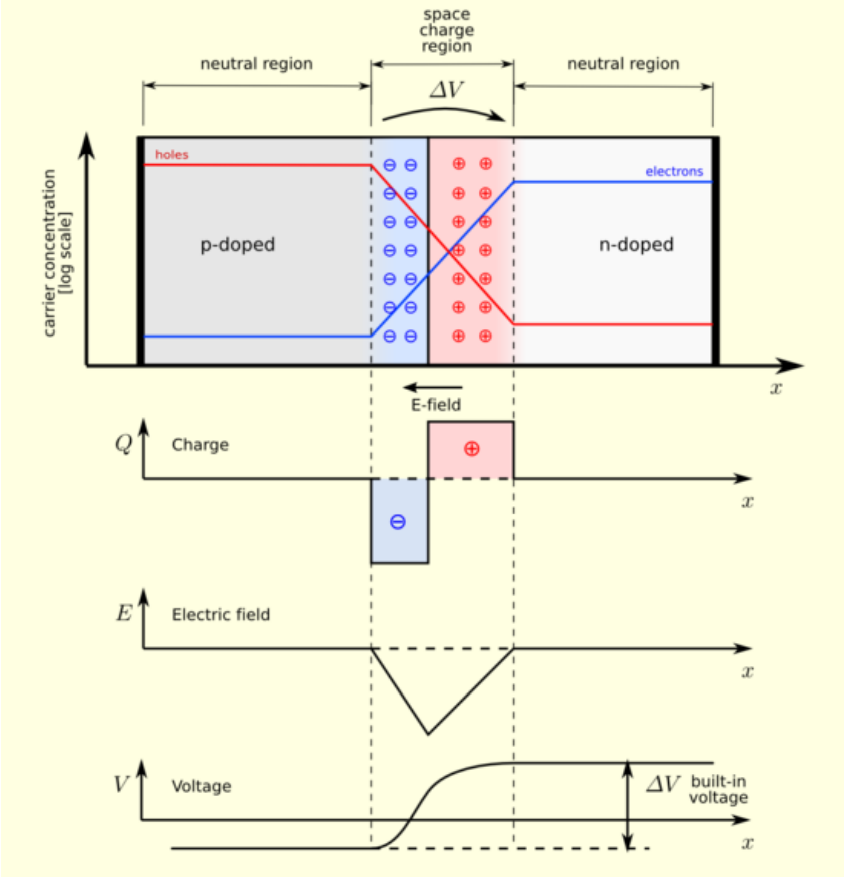

Forward/reverse biased (polarized)

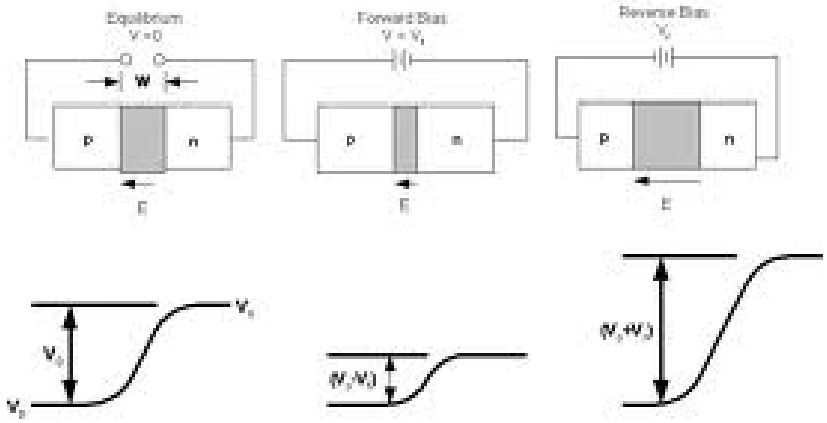

Current vs Voltage curve

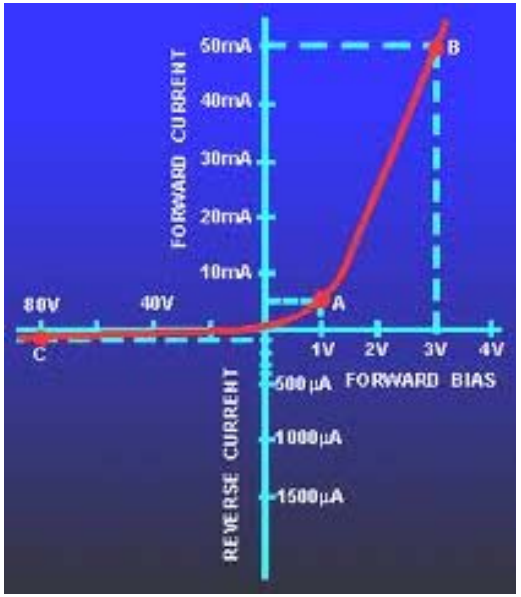

A p-n junction is realized at the interface between p- and n-doped semiconductor (e.g., Si)

PUMPING THE ACTIVE MEDIUM IN A DIODE

When forward-biased, electron and holes (negative and positive carriers) are both **injected** into the junction (from the negative and positive poles of the generator, respectively)

When an electron and a hole are found in close proximity each other, a **radiative recombination** may occur leading to "annihilation" of the pair into production of a photon

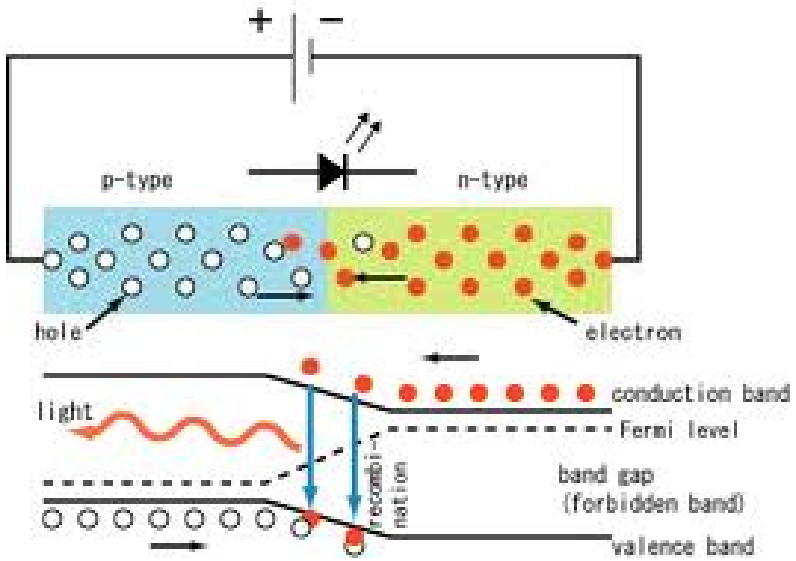

Somehow similar to excimer lasers, e-h recombination destroys the system

→ Population of the ground state is virtually null

→ Inversion of population (pumping) is *automatically* achieved

→ Pumping rate is controlled by the current

→ *Gain can be very large!*

✓ Indeed, electrons are injected into the conduction band and holes into the valence band

✓ This is equivalent to consider an excited quantum system, hence a pumped active medium

✓ For energy conservation, photons are emitted with an energy related to the band gap

SEMICONDUCTOR AND LIGHT EMISSION

In 3-D systems, e.g., bulk semiconductor crystals, the energy bands are not "flat" but depends on the electron wavevector (*energy dispersion*)

Bulk semiconductors, e.g., Si, are not suited because of energy gap (in the IR) and, mostly, **indirect transitions** strongly hampering the "quantum efficiency" of the radiative recombination

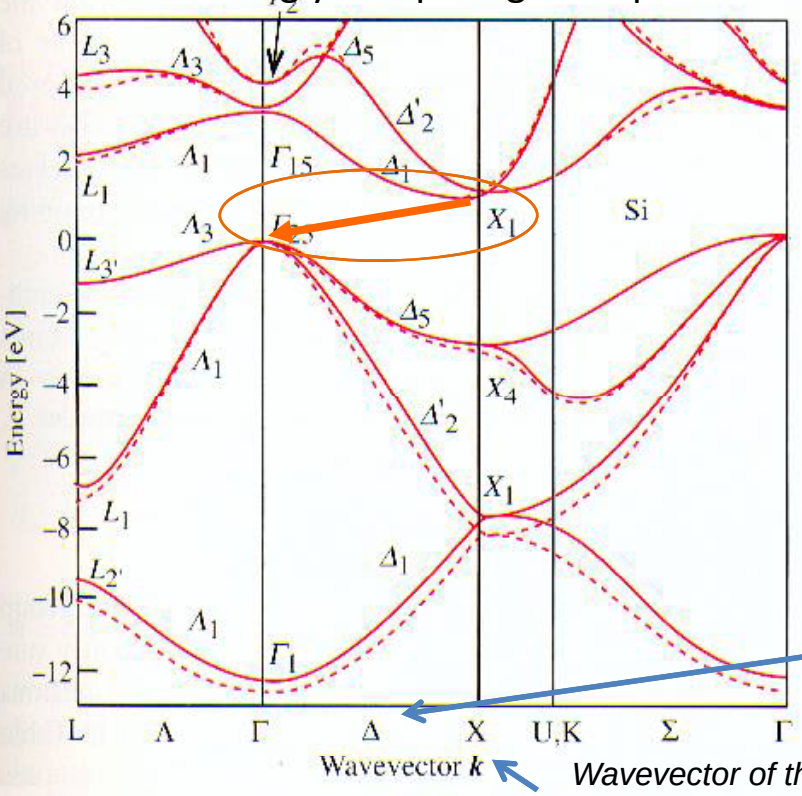

Band structure of Si

The top of valence band and the bottom of the conduction band are displaced each other in terms of electron wavevector

⇩

Momentum conservation implies phonons to be involved in the absorption process

⇩

Transition probability is small (10^{-5}-10^{-6} s^{-1}) (and wavelength is in the IR, above 1 ⌈m)

Special directions in the wavevector space, related to directions of symmetry in the (complicated) crystalline structure of Si

Wavevector of the electrons

Fig. 2.10. Electronic band structure of Si calculated by the pseudopotential technique. The *solid* and the *doted lines* represent calculations with a **nonlocal** and a **local pseudopotential**, respectively. [Ref. 2.6, p. 81]

Bulk semiconductive materials with indirect gap can be hardly used in electroluminescent devices

SEMICONDUCTOR ALLOYS I

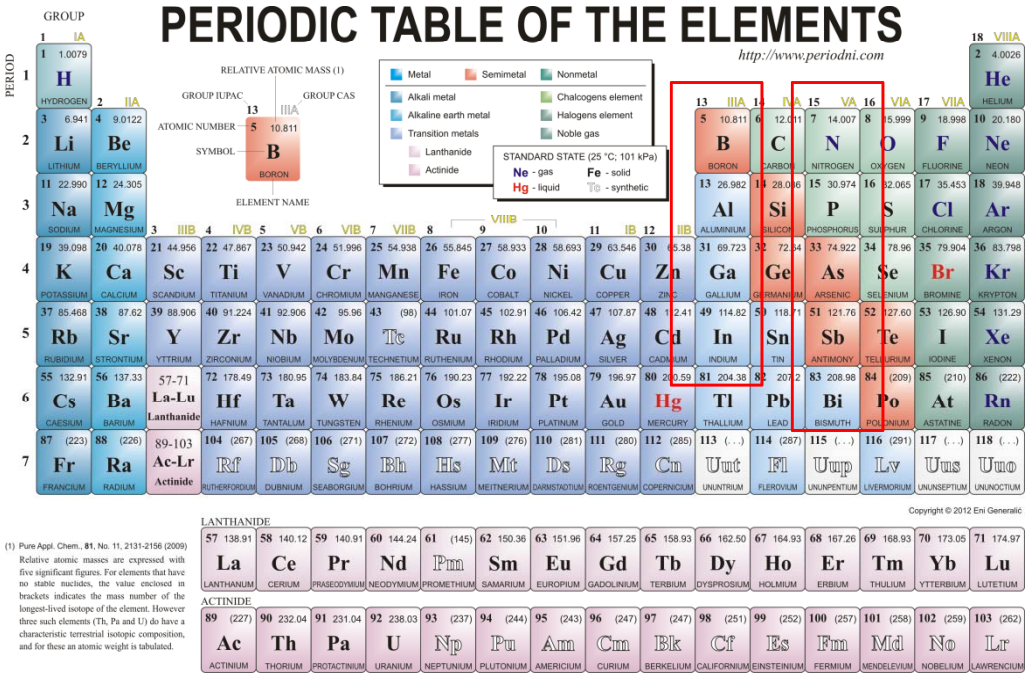

Luckily, it is possible to (artificially, mostly) produce **semicondcutive alloys**

Typically, elements of columns III and V of the periodic table can be stably alloyed to attain semiconductors with a certain gap energy, e.g., **GaAs** and **GaAlAs** (first alloys to be used in this context)

Such alloys can be doped, similar to Si or other elemental semiconductors

Note: alloy stability requires “structural affinity”, i.e., similar lattice constants

SEMICONDUCTOR ALLOYS II

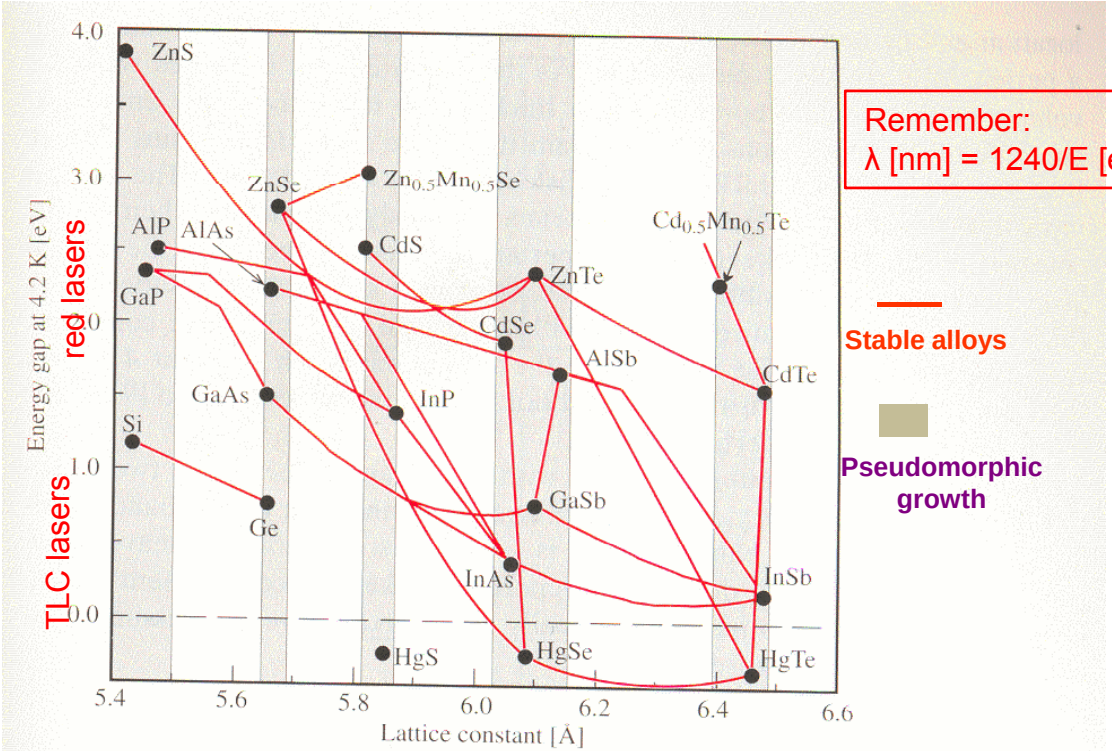

Fig. 9.2. A plot of the low temperature energy bandgaps of a number of semiconductors with the diamond and zinc-blende structure versus their lattice constants. The *shaded regions* highlight several families of semiconductors with similar lattice constants. Semiconductors joined by *solid lines* form stable alloys. [Chen A.B., Sher A.: *Semiconductor Alloys* (Plenum, New York 1995) Plate 1]

Remember:
λ [nm] = 1240/E [eV]

At some extent, the band gap energy can be "engineered" to meet specific wavelength requirements

Larger gaps achieved with GaN

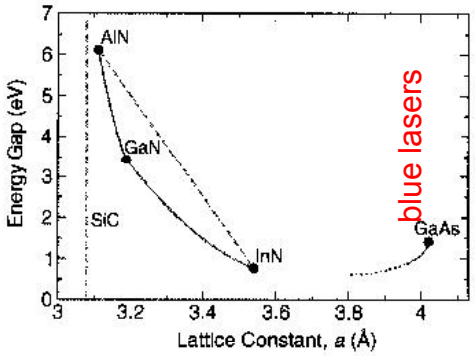

Figure 1. Fundamental bandgap versus basal-plane lattice constant of nitride materials compared with SiC and GaAs. The solid curves represent the ternary mixtures AlN/GaN,[10] GaN/InN,[11] and GaN/GaAs.[12] The dotted curve qualitatively indicates the continuation of the GaNAs gap toward GaN.

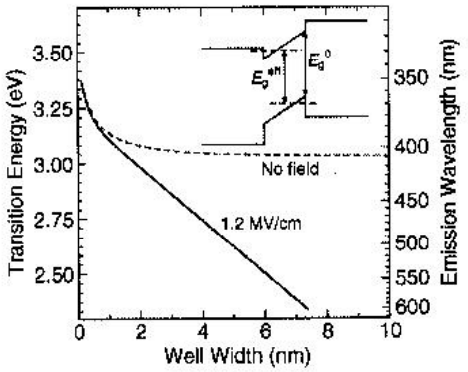

Figure 3. Transition energy of $Ga_{0.9}In_{0.1}N$/GaN quantum wells versus well width, with and without built-in electric field. The inset shows a schematic view of the band scheme, the effective bandgap E_g^{eff}, and the original bandgap E_g^0.

DIRECT TRANSITIONS IN ALLOYS

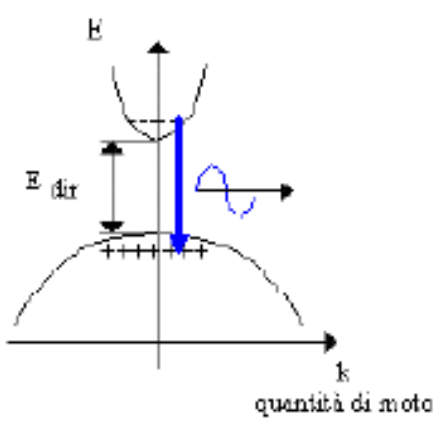

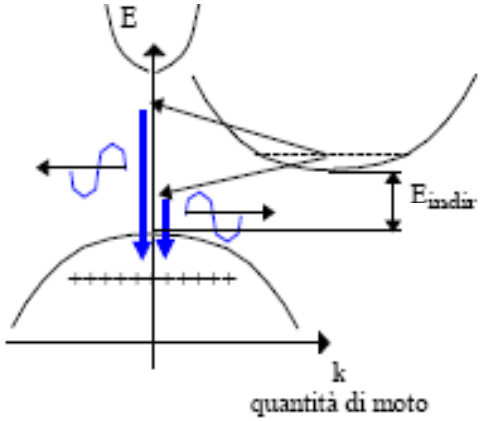

Most III-V alloys show **direct transition**

"Quantum efficiency" much larger than for, e.g., Si!

Materiali	Salto energetico [ev]	Tipo
GaN	3,5	diretto
SiN	2,8÷3,2	indiretto
$Al_XGa_{1-X}P$	2,26÷2,45	indiretto
Ga AS	1,44	diretto
GaP	2,26	indiretto
AlAs	2,16	indiretto
$In_{1-X}Ga_XP$	1,34÷2,26	dir-indiretto
$In_{1-X}Al_XP$	1,34÷2,45	dir-indiretto
$Al_XGa_{1-X}As$	1,44÷2,16	dir-indiretto
$GaAs_{1-X}P_X$	1,44÷2,26	dir-indiretto

The band gap energy can be (slightly) tuned also by playing with the alloy concentration

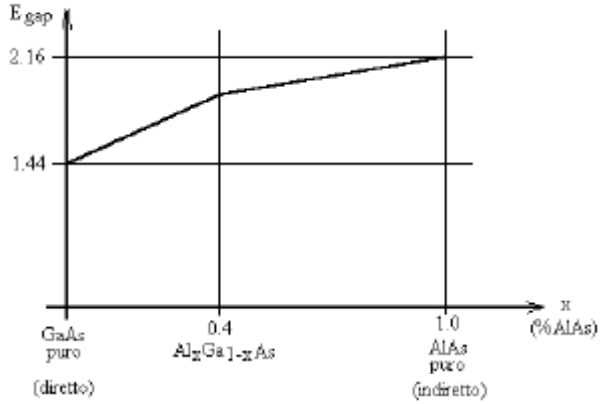

HOMOJUCNTION LASER (OLD!)

For Hall, who already had extensive experience with GaAs alloy junctions, tunnel diodes, and light-emitting diodes, the project to make a laser diode was an extension of his prior research work. It also coupled well with his optical experience in his earlier youthful hobbyist efforts to build telescopes and to polish lenses and mirrors [3]. Hall's laser project team included Dick Carlson, Gunther Fenner, Jack Kingsley, and Ted Soltys. Whereas other groups thinking about semiconductor lasers had proposed to use a macroscopic "external cavity" into which a GaAs diode was placed, Hall decided to polish parallel faces onto his GaAs diodes so that the Fabry- Perot optical cavity geometry was built into the device. This approach was not universally applied and, in fact, the importance of optical feedback into the diode "active region" was not fully appreciated by many workers. Hall's team operated their first successful GaAs laser diodes under pulsed conditions at 77K on September 16, 1962 [1]. A schematic diagram of Hall's early concept for an injection laser is

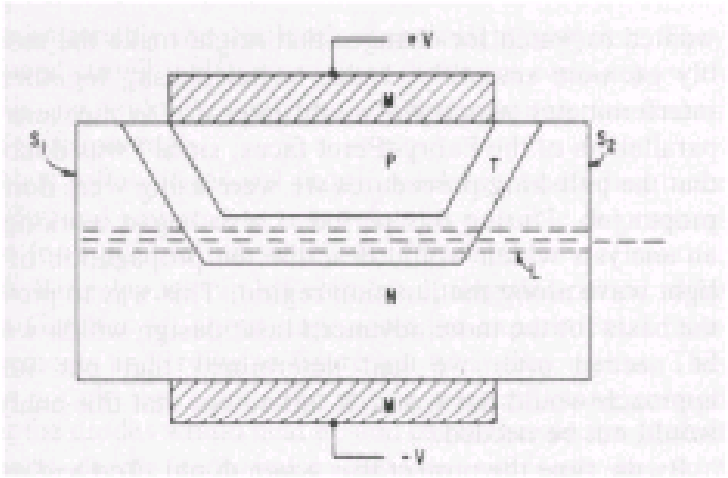

Figure 1: Schematic diagram of initial concept for an injection laser developed at General Electric Research Laboratories by Robert Hall in 1962.

Homojunction: n- and p-doped GaAs

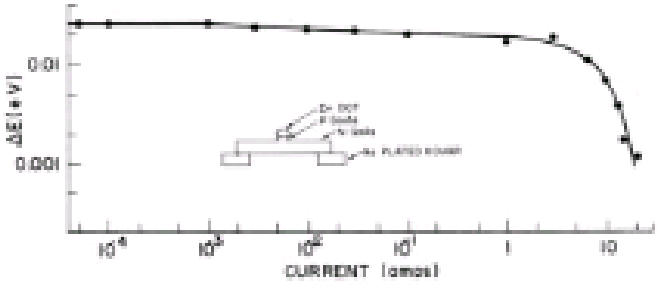

Figure 2: Spectral linewidth vs. current for a GaAs diode made at IBM and operated at 77K. The diode did not have a Fabry-Perot geometry so cavity modes were not observed.

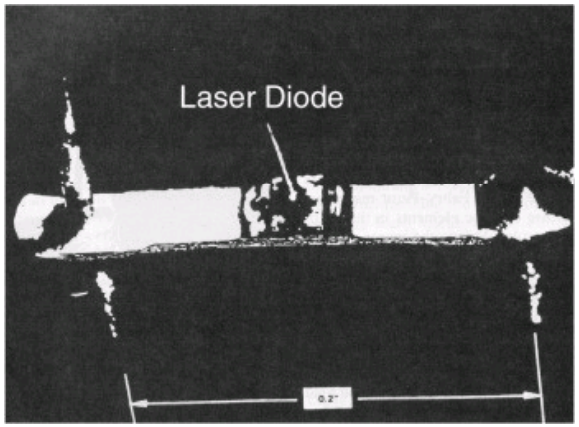

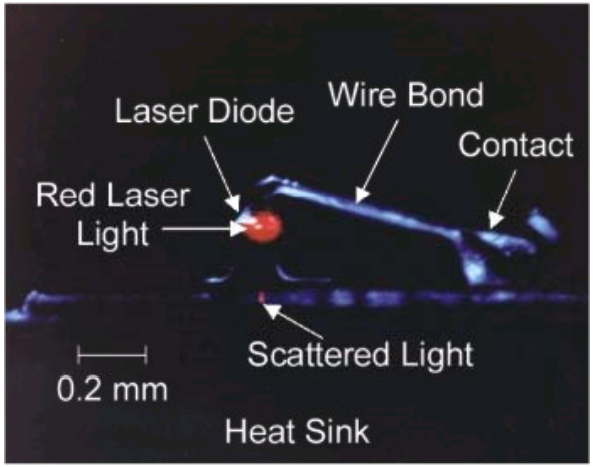

Demonstrated in the '60s, but very cumbersome and not efficient

REFLECTION AT THE INTERFACE

When light moves from a medium of a given refractive index n_1 into a second medium with refractive index n_2, both reflection and refraction of the light may occur.

In the diagram on the right, an incident light ray **PO** strikes at point **O** the interface between two media of refractive indexes n_1 and n_2. Part of the ray is reflected as ray **OQ** and part refracted as ray **OS**. The angles that the incident, reflected and refracted rays make to the normal of the interface are given as θ_i, θ_r and θ_t, respectively. The relationship between these angles is given by the law of reflection and Snell's law.

The fraction of the intensity of incident light that is reflected from the interface is given by the *reflection coefficient* R, and the fraction refracted by the *transmission coefficient* T. The Fresnel equations, which are based on the assumption that the two materials are both *non-magnetic*, may be used to calculate R and T in a given situation. The following fields are continuous: tangential E and H, normal B and D.

The calculations of R and T depend on polarisation of the incident ray. If the light is polarised with the electric field of the light perpendicular to the plane of the diagram

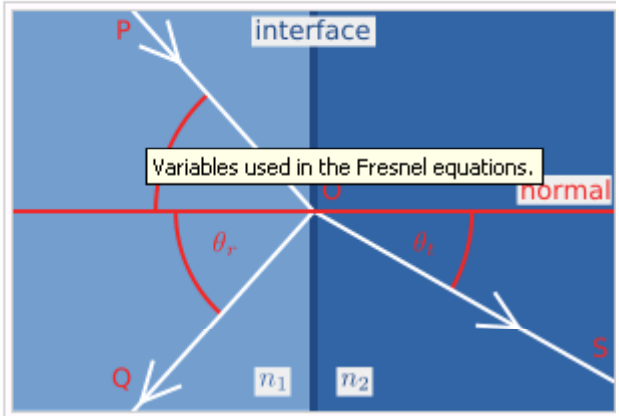

Variables used in the Fresnel equations.

$$R_s = \left[\frac{\sin(\theta_t - \theta_i)}{\sin(\theta_t + \theta_i)}\right]^2 = \left[\frac{n_1\cos(\theta_i) - n_2\cos(\theta_t)}{n_1\cos(\theta_i) + n_2\cos(\theta_t)}\right]^2 = \left[\frac{n_1\cos(\theta_i) - n_2\sqrt{1-\left(\frac{n_1}{n_2}\sin\theta_i\right)^2}}{n_1\cos(\theta_i) + n_2\sqrt{1-\left(\frac{n_1}{n_2}\sin\theta_i\right)^2}}\right]^2$$

where θ_t can be derived from θ_i by Snell's law and is simplified using trigonometric identities.

If the incident light is polarised in the plane of the diagram (*p*-polarised), the R is given by:

$$R_p = \left[\frac{\tan(\theta_t - \theta_i)}{\tan(\theta_t + \theta_i)}\right]^2 = \left[\frac{n_1\cos(\theta_t) - n_2\cos(\theta_i)}{n_1\cos(\theta_t) + n_2\cos(\theta_i)}\right]^2 = \left[\frac{n_1\sqrt{1-\left(\frac{n_1}{n_2}\sin\theta_i\right)^2} - n_2\cos(\theta_i)}{n_1\sqrt{1-\left(\frac{n_1}{n_2}\sin\theta_i\right)^2} + n_2\cos(\theta_i)}\right]^2$$

The transmission coefficient in each case is given by $T_s = 1 - R_s$ and $T_p = 1 - R_p$.

If the incident light is unpolarised (containing an equal mix of *s*- and *p*-polarisations), the reflection coefficient is $R = (R_s + R_p)/2$.

When the light is at near-normal incidence to the interface (θ_i

$$R = R_s = R_p = \left(\frac{n_1 - n_2}{n_1 + n_2}\right)^2$$

$$T = T_s = T_p = 1 - R = \frac{4n_1n_2}{(n_1 + n_2)^2}$$

GaAs: n~3.7
→ $R_{orthogonal}$~0.33

Few interest for designing an optical cavity in the first diode laser…
End mirrors (plane parallel) just made by the interface between semiconductor and air

LIMITS OF HOMOJUNCTION LASERS I

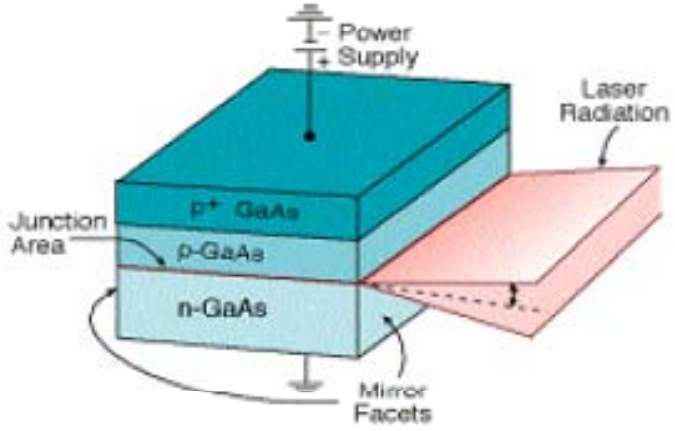

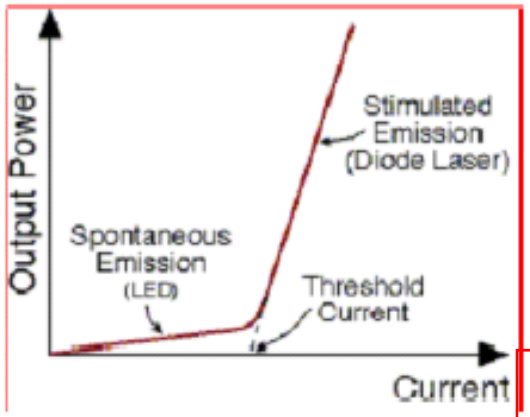

These layers of semiconductor materials are arranged such that at the p-n junction an active region is created, in which photons are created by the recombination process. On the top and bottom layers, a layer of metal allows connecting external voltage to the laser. The voltage is applied to metal contacts above and below the semiconductor layers. The side of the crystalline semiconductor are cut to serve as mirrors at the end of the optical cavity.

The radiation comes out of a rectangular shape of a very thin active layer, and spreads at different angles in 2 directions.

If the condition of population inversion does not exist, the photons will be emitted by spontaneous emission. These photons will be emitted randomly in all directions, that is the basis of operation of a light emitting diode (LED). The condition for population inversion depends on the pumping. By increasing the current injected through the p-n junction, we arrive at threshold current, which fulfills this condition.It is easily seen that the slope of this graph in a stimulated emission (laser) is far greater than the slope at spontaneous emission (LED).

The threshold current for lasing is determined by the intercept of the tangent to the graph at stimulated emission with the current axis (this point is very close to the point of change in the slope). When the current threshold is low, less energy will be wasted in the form of heat, and more energy will be transmitted as laser radiation. Practically, the important parameter is current density (A/cm^2).

Radiative recombination requires proximity of e-h pairs

⇓

Only a very thin layer at the junction is interested by lasing

⇓

Huge threshold current density (and short lifetime)

End mirrors with poor reflectivity (and quality)

⇓

Small *Q-factor*, small efficiency

LIMITS OF HOMOJUNCTION LASERS II

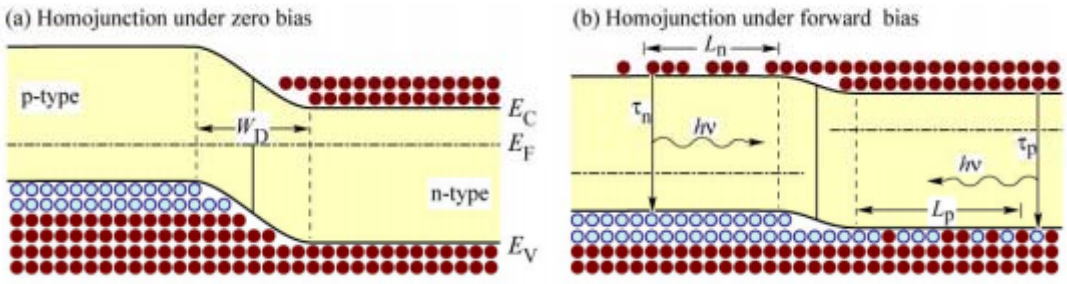

In other words: the inversion of population is realized only in a thin layer (**inversion layer**) within the junction

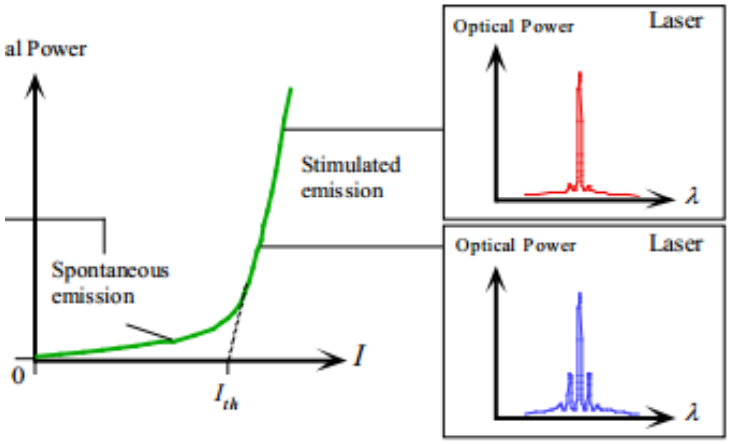

The drawback of a homojunction diode laser is the high threshold current density therefore it is restricted to operating at very low temperatures or pulsed mode

1000 A/cm^2 at 77 K temperatures

100 000 A/cm^2 at 300 K temperatures

Too poor efficiency (and too prone to damage) for practical use!

TECHNOLOGICAL PROGRESSES

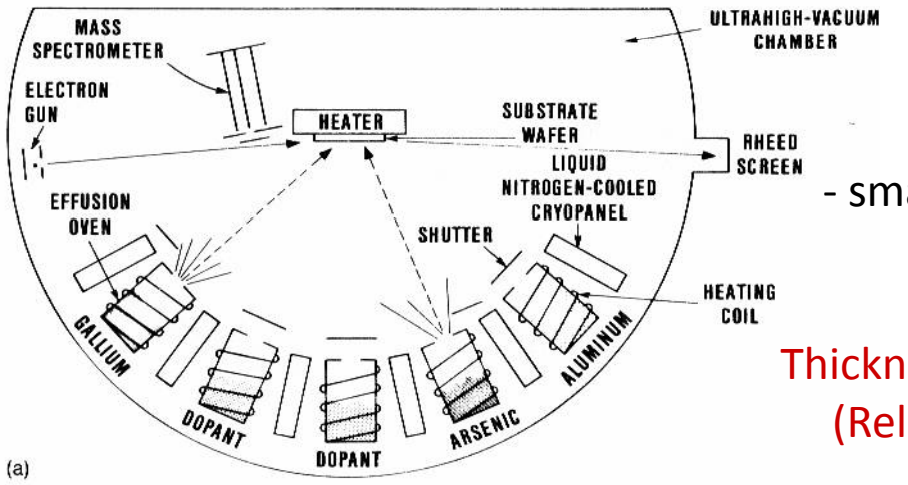

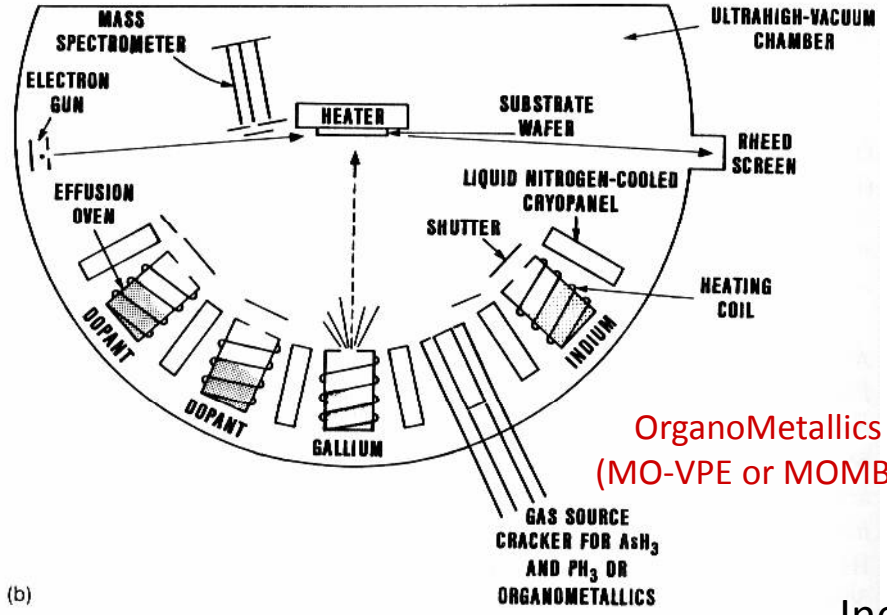

Key points for MBE:

- clean process (UHV, $p \leq 10^{-10}$mbar)
- small continuous deposition rate (~ 1 µm/h)
- suitable with semiconductor

⇩

Thickness easily controlled at the monolayer level

(Relatively) low kinetic energy favors epitaxy

Heterostructures easily fabricated

OrganoMetallics
(MO-VPE or MOMBE)

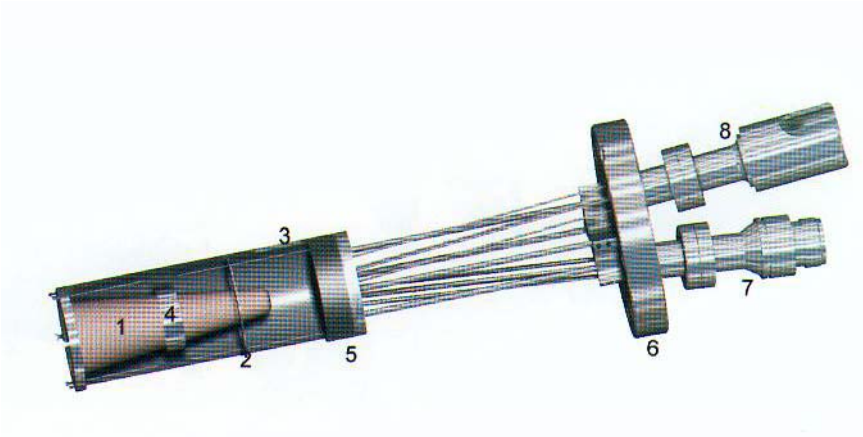

Example of effusive oven (MPI)

Inert materials used (but difficult with oxides!)

HETEROSTRUCTURES

Heterostructures(superlattices): sequence of layers made of semiconductors with different gap energies

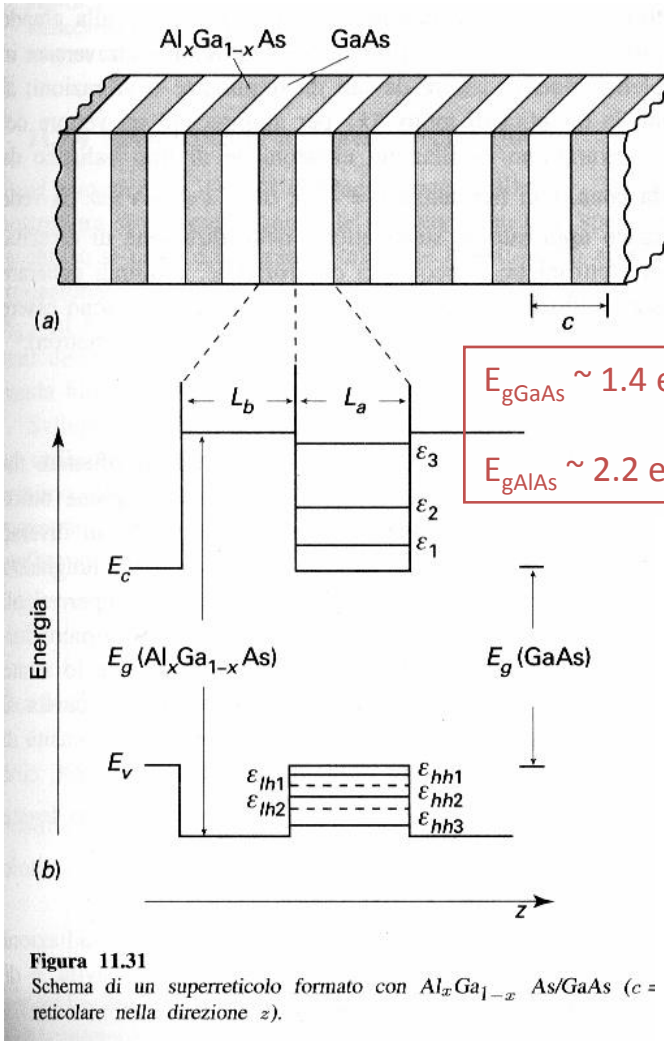

E_{gGaAs} ~ 1.4 eV

E_{gAlAs} ~ 2.2 eV

Figura 11.31
Schema di un superreticolo formato con Al_xGa_{1-x} As/GaAs (c = reticolare nella direzione z).

Da Bassani Grassano,
Fisica dello Stato Solido,
Boringhieri (2000)

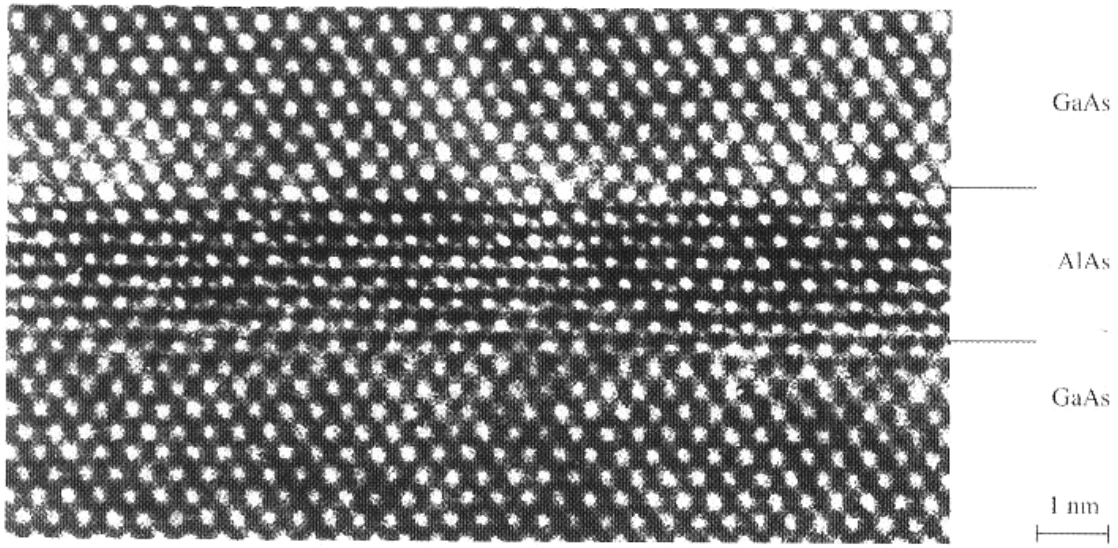

Fig. 9.1. High resolution transmission electron micrograph (TEM) showing a GaAs/AlAs superlattice for a [110] incident beam. (Courtesy of K. Ploog, Paul Drude Institute, Berlin.) In spite of the almost perfect interfaces, try to identify possible Al atoms in Ga sites and vice versa

MULTIPLE QUANTUM WELLS (MQWs)

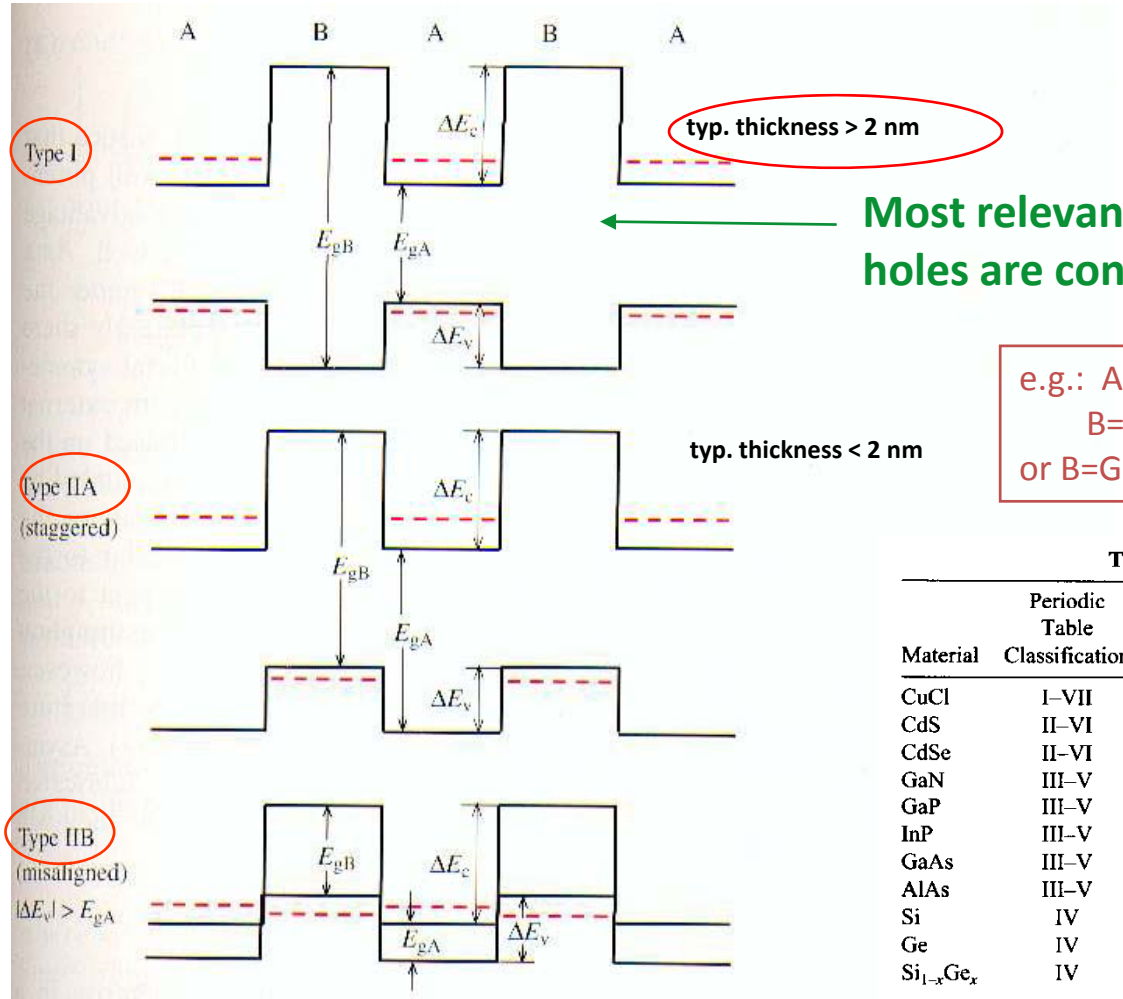

typ. thickness > 2 nm

typ. thickness < 2 nm

Most relevant configuration: electrons and holes are confined in the same layer

e.g.: A=GaAs (E_{gA} ~ 1.4 eV, lattice 5.653 Å)
B=AlAs (E_{gB} ~ 2.2 eV, lattice 5.62 Å)
or B=$Ga_{1-x}Al_xAs$ (x typ. ≤ 0.3)

Fig. 9.3. Schematic diagrams of three arrangements of the confinement holes in MQWs and superlattices formed by two semiconductors A and E_{gA} and E_{gB}, respectively. In type I samples both the electrons and holes are confined in the same layer A. The energies of the confined particles are represented by *red lines*. In type IIA systems the electrons and holes are confined in different layers. Type IIB samples are a special case of type IIA behavior. They are either small gap semiconductors or semimetals

Table 4.1. Semiconductor Material Parameters

Material	Periodic Table Classification	Bandgap Energy (eV)	Bandgap Wavelength (μm)	Exciton Bohr Radius (nm)	Exciton Binding Energy (meV)
CuCl	I–VII	3.395	0.36	0.7	190
CdS	II–VI	2.583	0.48	2.8	29
CdSe	II–VI	1.89	0.67	4.9	16
GaN	III–V	3.42	0.36	2.8	
GaP	III–V	2.26	0.55	10–6.5	13–20
InP	III–V	1.35	0.92	11.3	5.1
GaAs	III–V	1.42	0.87	12.5	5
AlAs	III–V	2.16	0.57	4.2	17
Si	IV	1.11	1.15	4.3	15
Ge	IV	0.66	1.88	25	3.6
$Si_{1-x}Ge_x$	IV	$1.15–0.874x + 0.376x^2$	$1.08–1.42x + 3.3x^2$	$0.85–0.54x + 0.6x^2$	$14.5–22x + 20x^2$
PbS	IV–VI	0.41	3	18	4.7
AlN	III–V	6.026	0.2	1.96	80

MQW II

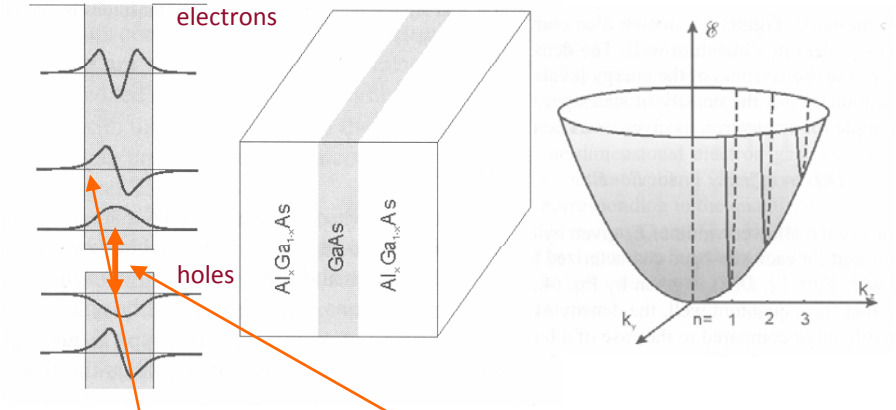

- For energies $E < V$, the energy levels of the electron are quantized for the direction z of the confinement; hence they are given by the model of particle in a one-dimensional box. The electronic energies in the other two dimensions (x and y) are not discrete and are given by the effective mass approximation discussed in Chapter 2. Therefore, for $E < V$, the energy of an electron in the conduction band is given as

$$E_{n,k_x,k_y} = E_C + \frac{n^2\hbar^2}{8m_e^* l^2} + \frac{\hbar^2(k_x^2 + k_y^2)}{2m_e^*} \qquad (4.1)$$

where $n = 1, 2, 3$ are the quantaum numbers. The second term on the right-hand side represents the quantized energy; the third term gives the kinetic energy of the electron in the x–y plane in which it is relatively free to move. The symbols used are as follows: m_e^* is the effective mass of electron, and E_C is the energy corresponding to the bottom of the conduction band.

Equation (4.1) shows that for each quantum number n, the values of wavevector components k_x and k_y form a two-dimensional band structure. However, the wavevector k_z along the confinement direction z takes on only discrete values, $k_z = n\pi/l$. Each of the bands for a specific value of n is called a sub-band. Thus n becomes a sub-band index. Figure 4.2 shows a two-dimensional plot of these sub-bands.

- For $E > V$, the energy levels of the electron are not quantized even along the z direction. Figure 4.1 shows that for the AlGaAs/GaAs quantum well, the quantized levels $n = 1$–3 exist, beyond which the electronic energy level is a continuum. The total number of discrete levels is determined by the width l of the well and the barrier height V.

- The holes behave in analogous way, except their quantized energy is inverted and the effective mass of a hole is different. Figure 4.1 also shows that for the holes, two quantized states with quantum numbers $n = 1$ and 2 exist for this particular quantum well (determined by the composition of AlGaAs and the width of the well). In the case of the GaAs system, two types of holes exist, determined by the curvature (second derivative) of the band structure. The one with a smaller effective mass is called a *light hole* (lh), and the other with a heavier effective mass is called a *heavy hole* (hh). Thus the $n = 1$ and $n = 2$ quantum states actually are each split in two, one corresponding to lh and the other to hh.
- Because of the finite value of the potential barrier ($V \neq \infty$), the wavefunctions, as shown for levels $n = 1, 2$, and 3 in the case of electrons and levels $n = 1$ and 2 in the case of holes, do not go to zero at the boundaries. They extend into the region of the wider bandgap semiconductor, decaying exponentially into this region. This electron leakage behavior has already been discussed in Section 2.1.3 of Chapter 2.
- The lowest-energy band-to-band optical transition (called the interband transition) is no longer at E_g, the energy gap of the smaller bandgap semiconductor, GaAs in this case. It is at a higher energy corresponding to the difference between the lowest energy state ($n = 1$) of the electrons in the conduction band and the corresponding state of the holes in the valence band. The effective bandgap for a quantum well is defined as

$$E_g^{\text{eff}} = (E_C - E_V) + \frac{\hbar^2}{8l^2}\left(\frac{1}{m_e^*} + \frac{1}{m_h^*}\right) \qquad (4.2)$$

In addition, there is an excitonic transition below the band-to-band transition. These transitions are modifications of the corresponding transitions found for a bulk semiconductor. In addition to the interband transitions, new transitions between the different sub-bands (corresponding to different n values) within the conduction band can occur. These new transitions, called intraband or inter-sub-band transitions, find important technologic applications such as in quantum cascade lasers. The optical transitions in quantum-confined structures are further discussed in the next section.

Da P.N. Prasad,
Nanophotonics,
Wiley (2004)

MQW III

- Another major modification, introduced by quantum confinement, is in the density of states. The density of states $D(E)$, defined by the number of energy states between energy E and $E + dE$, is determined by the derivative $dn(E)/dE$. For a bulk semiconductor, the density of states $D(E)$ is given by $E^{1/2}$. For electrons in a bulk semiconductor, $D(E)$ is zero at the bottom of the conduction band and increases as the energy of the electron in the conduction band increases. A similar behavior is exhibited by the hole, for which the energy dispersion (valence band) is inverted. Hence, as the energy is moved below the valence band maximum, the hole density of states increases as $E^{1/2}$. This behavior is shown in Figure 4.3, which also compares the density of states for electrons (holes) in a quantum well. The density of states is a step function because of the discreteness of the energy levels along the z direction (confinement direction). Thus the density of states per unit volume for each sub-band, for example for an electron, is given as a rise in steps of

$$D(E) = m_e^*/\pi^2 \qquad \text{for } E > E_1 \tag{4.3}$$

The steps in $D(E)$ occur at each allowed value of E_n given by Equation (4.1), for k_x and $k_y = 0$, then stay constant for each sub-band characterized by a specific n (or k_z). For the first sub-band with $E_n = E_1$, $D(E)$ is given by Eq. (4.3). This step-like behavior of $D(E)$ implies that for a quantum well, the density of states in the vicinity of the bandgap is relatively large compared to the case of a bulk semiconductor for which $D(E)$ vanishes. As is discussed below, a major manifestation of this modification of the density of states is in the strength of optical transition. A major factor in the expression for the strength of optical transition (often defined as the oscillator strength) is the density of states. Hence, the oscillator strength in the vicinity of the bandgap is considerably enhanced for a quantum well compared to a bulk semiconductor. This enhanced oscillator strength is particularly important in obtaining laser action in quantum wells, as discussed in Section 4.4.

DOS

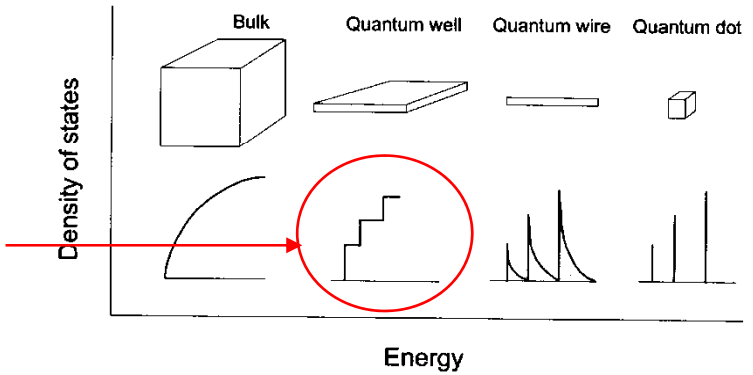

Figure 4.3. Density of states for electrons in bulk conduction band together with those in various confined geometries.

Optical transitions in quantum confined systems

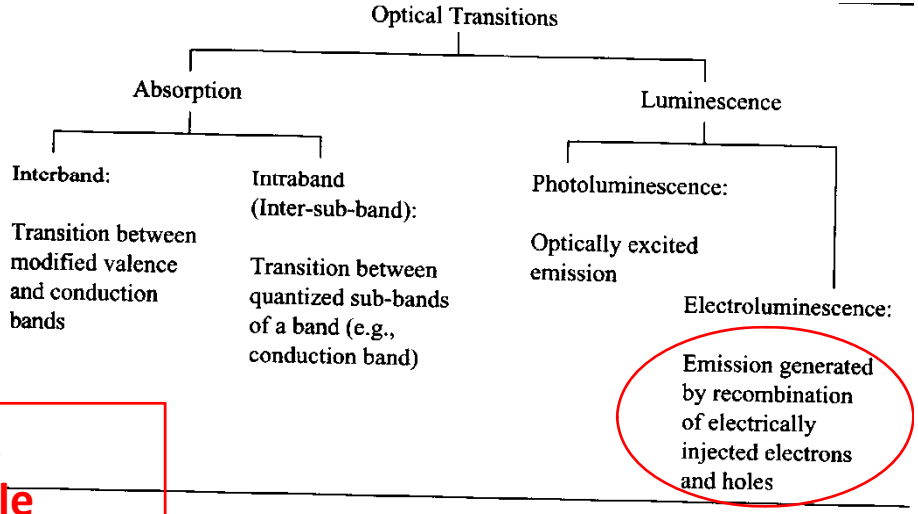

- ✓ **Interband transition energy is no longer E_{GAP}**
- ✓ **Intraband (intersubband) transitions available**
- ✓ **Increased transition "strength" (oscillator strength)**

EXCITONS (A FEW WORDS)

Whenever electron and hole wavefunctions overlap each other, a quasi-bound system can be formed called **exciton**

Il calcolo dell'energia di legame degli eccitoni può essere effettuato in modo analogo a quello delle impurezze nei semiconduttori se le bande di valenza e di conduzione sono sferiche e non degeneri. Analogamente a quanto visto nel cap. 11, si ricava che i livelli idrogenoidi (riferiti alla cima della banda di valenza) hanno energie date da:

Hydrogen-like energy levels!

$$E_n = E_g - \frac{\mu e^4}{2\hbar^2 \varepsilon^2} \frac{1}{n^2}, \qquad (12.107)$$

ove n è il numero quantico principale, ε la costante dielettrica, e μ la massa ridotta del complesso elettrone-buca

$$\frac{1}{\mu} = \frac{1}{m_e^*} + \frac{1}{m_h^*} \cdot \qquad (12.108)$$

Nei semiconduttori abbiamo visto che $\varepsilon \simeq 10$ e $\mu \simeq 0.5 m_e$, per cui l'energia di legame degli eccitoni sarà dell'ordine di qualche decina di meV. A causa della grande costante dielettrica l'eccitone è dunque debolmente legato e la distanza media elettrone-buca è dell'ordine di decine di distanze reticolari. Un eccitone con queste caratteristiche è chiamato eccitone di Wannier-Mott, e ne discuteremo

Electron and hole system bound by Coulomb forces

⇩

Exciton behaves like an hydrogen atom (but for some degeneracy removal, e.g., light and heavy hole states)

In (type I) quantum wells there is a high probability of exciton formation due to confinement of electrons and holes in the same layer

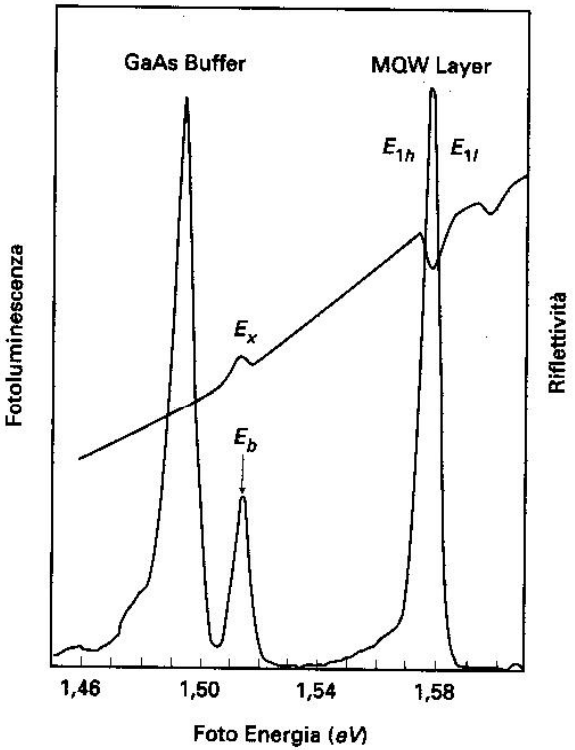

Figura 12.28
Fluorescenza eccitonica da un pozzo quantico (Q.W.) GaAs/$Ga_{1-x}Al_xAs$ e dal substrato GaAs a 12 K. E_b indica la posizione dell'eccitone nel substrato, E_{1h} ed E_{1l} gli eccitoni di buca pesante e di buca leggera nel Q.W. Per confronto è riportata anche la riflettività. Il picco di buca leggera compare soltanto ad alte temperature in fluorescenza, mentre è visibile in riflettività. (Da Y. Chen, R. Cingolani, L.C. Andreani, F. Bassani e J. Massies, Il Nuovo Cimento **D10**, 847 (1988)).

HETEROJUNCTION LASER I

The use of heterostructures enables realization of heterojunction lasers with the double aim of:

1. ***Carrier confinement:*** Confine the injected electrons and holes to a narrow region about the junction. This requires less current to establish the required concentration of electrons for population inversion.

2. ***Photon confinement:*** Construct a dielectric waveguide around the optical gain region to increase the photon concentration and elevate the probability of stimulated emission. This reduces the number of electrons lost traveling off the cavity axis.

Double heterostructure laser

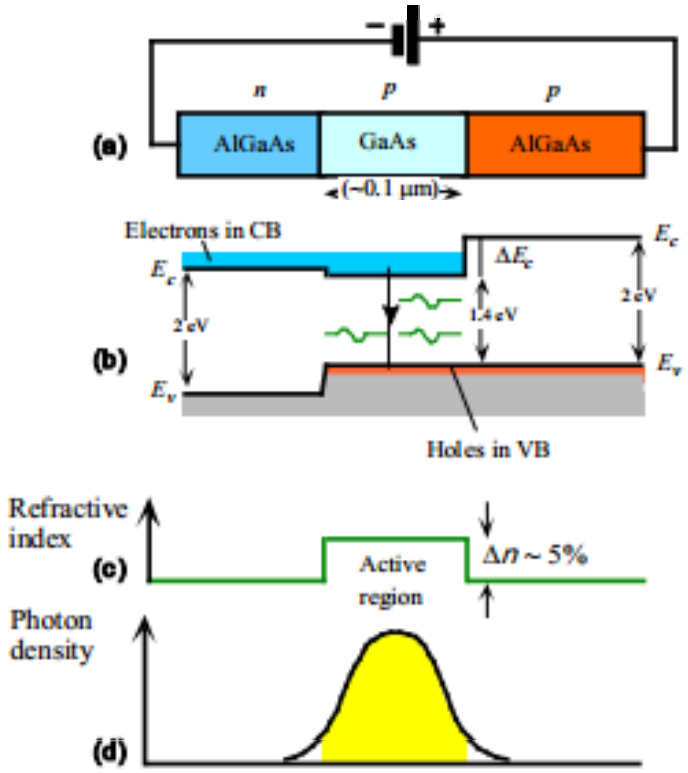

(a) A double heterostructure diode has two junctions which are between two different bandgap semiconductors (GaAs and AlGaAs).

(b) Simplified energy band diagram under a large forward bias. Lasing recombination takes place in the *p*-GaAs layer, the *active layer*

(c) Higher bandgap materials have a lower refractive index

(d) AlGaAs layers provide lateral optical confinement.

1

Inversion of population occurs in a predefined region (the p-doped GaAs layer, in this case)

Pumping efficiency is greatly enhanced

2

Thanks to the refractive index variation, photons are confined into the active layer (a cavity is realized) n this case)

Q-factor is improved

HETEROJUNCTION LASER II

1. Due to the thin p-GaAs layer a minimal amount of current is required to increase the concentration of injected carriers. This is how the threshold current for population inversion and optical gain is reduced

2. The semiconductor with a wider bandgap (AlGaAs) will also have a lower refractive index than GaAs. This difference in refractive index is what establishes an optical dielectric waveguide that ultimately confines photons to the active region

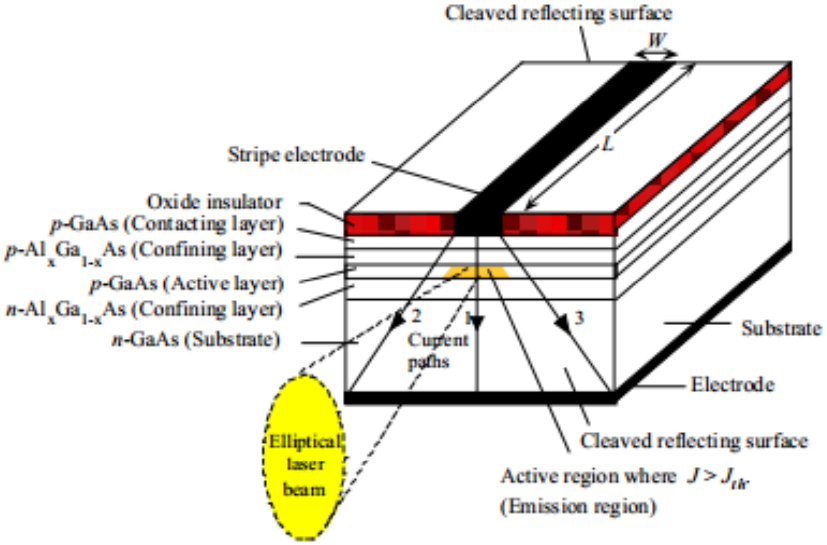

Schematic illustration of the the structure of a double heterojunction stripe contact laser diode

The quality of the cavity, that is the quality of the end mirrors, relies essentially on the correct cleavage of the facets

In any case, unstable resonators are obtained with large losses ("balanced" by the high gain, though)

HETEROJUNCTION LASER III

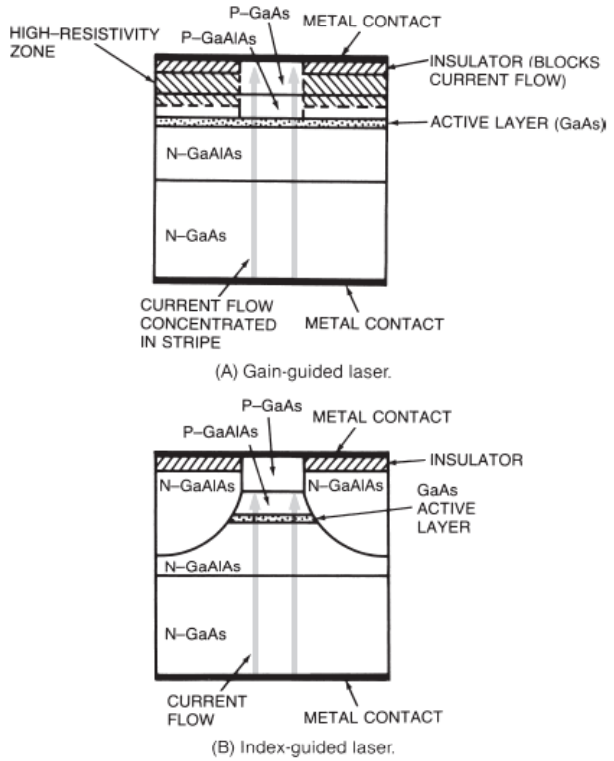

Figure 9-12. End views of gain-guided and index-guide

Further improvements of the efficiency (intended as lower threshold current and slightly enhanced optical properties) can be achieved by confining photons and electrons also in the in-plane direction

- Gain guided (electrons are injected only in the center of the junction)
- Index guided (a refractive index modulation in the in-plane direction leads to photon confinement)

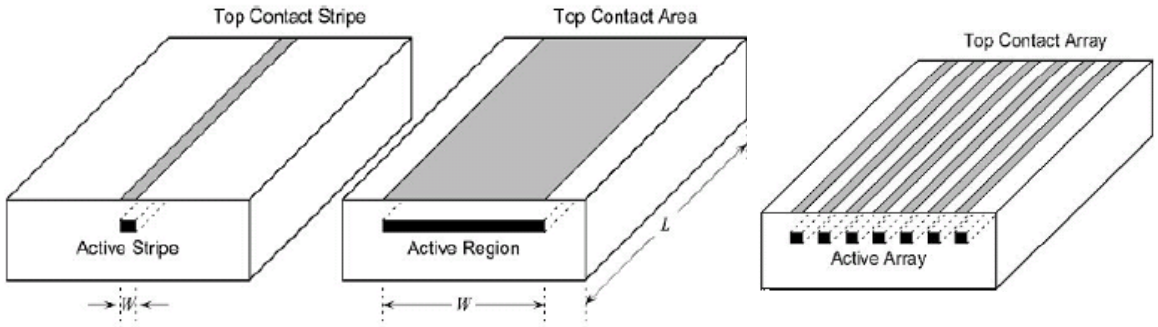

Typical power of a GaAs/GaAlAs laser is below 200 mW, but large stripe and, especially, bar diode laser can produce up to several tens of W in cw operation (at the expenses of the optical quality, awful…)

RATE EQUATIONS FOR DIODE LASERS I

The laser diode rate equations model the electrical and optical performance of a laser diode. This system of ordinary differential equations relates the number or density of photons and charge carriers (electrons) in the device to the injection current and to device and material parameters such as carrier lifetime, photon lifetime, and the optical gain.

The rate equations may be solved by numerical integration to obtain a time-domain solution, or used to derive a set of steady state or small signal equations to help in further understanding the static and dynamic characteristics of semiconductor lasers.

The laser diode rate equations can be formulated with more or less complexity to model different aspects of laser diode behavior with varying accuracy.

Multimode rate equations [edit]

In the multimode formulation, the rate equations model a laser with multiple optical modes. This formulation requires one equation for the carrier density, and one equation for the photon density in each of the optical cavity modes:

$$\frac{dN}{dt} = \frac{I}{eV} - \frac{N}{\tau_n} - \sum_{\mu=1}^{\mu=M} G_\mu P_\mu$$

$$\frac{dP_\mu}{dt} = \Gamma_\mu (G_\mu - \frac{1}{\tau_p}) P_\mu + \beta_\mu \frac{N}{\tau_n}$$

The pumping rate is introduced as the number of carriers injected into the junction

where:

M is the number of modes modelled, μ is the mode number, and subscript μ has been added to G, Γ, and β to indicate these properties may vary for the different modes.

Spectral Shift [edit]

Dynamic wavelength shift in semiconductor lasers occurs as a result of the change in refractive index in the active region during intensity modulation. It is possible to evaluate the shift in wavelength by determining the refractive index change of the active region as a result of carrier injection. A complete analysis of spectral shift during direct modulation found that the refractive index of the active region varies proportionally to carrier density and hence the wavelength varies proportionally to injected current.

Experimentally, a good fit for the shift in wavelength is given by:

$$\delta\lambda = k\left(\sqrt{\frac{I_0}{I_{th}}} - 1\right)$$

where I_0 is the injected current and I_{th} is the lasing threshold current.

The injection of current can modify the refractive index of the active medium → the free spectral range of the cavity → current-driven wavelength shifts

RATE EQUATIONS FOR DIODE LASERS I

The modal gain [edit]

G_μ, the gain of the μ^{th} mode, can be modelled by a parabolic dependence of gain on wavelength as follows:

$$G_\mu = \frac{\alpha N[1-(2\frac{\lambda(t)-\lambda_\mu}{\delta\lambda_g})^2]-\alpha N_0}{1+\epsilon\sum_{\mu=1}^{\mu=M}P_\mu}$$

where: α is the gain coefficient and ε is the gain compression factor (see below). λ_μ is the wavelength of the μ^{th} mode, $\delta\lambda_g$ is the full width at half maximum (FWHM) of the gain curve, the centre of which is given by

$$\lambda(t) = \lambda_0 + \frac{k(N_{th}-N(t))}{N_{th}}$$

where λ_0 is the centre wavelength for $N = N_{th}$ and k is the spectral shift constant (see below). N_{th} is the carrier density at threshold and is given by

$$N_{th} = N_{tr} + \frac{1}{\alpha\tau_p\Gamma}$$

where N_{tr} is the carrier density at transparency.

β_μ is given by

$$\beta_\mu = \frac{\beta_0}{1+(2(\lambda_s-\lambda_\mu)/\delta\lambda_s)^2}$$

where

β_0 is the spontaneous emission factor, λ_s is the centre wavelength for spontaneous emission and $\delta\lambda_s$ is the spontaneous emission FWHM. Finally, λ_μ is the wavelength of the μ^{th} mode and is given by

$$\lambda_\mu = \lambda_0 - \mu\delta\lambda + \frac{(n-1)\delta\lambda}{2}$$

where $\delta\lambda$ is the mode spacing.

Modeling the behavior of a laser diode is typically a very hard task since:

- Pumping rate depends on the current density, i.e., on the carrier injected
- Refractive index, hence frequency filtering by the cavity, depends on the current
- *Moreover, any temperature change can cause thermal expansion leading to modify the optical beahvior as well*

AN EXAMPLE OF CHARACTERISTICS

Description

The SLD1135VS is a index-guided red laser diode for Laser pointer. The wavelength is 20nm shorter than SLD1122VS.

Features

- Small astigmatism (7μm typ.)
- Small package (ϕ5.6mm)
- Single longitudinal mode
- Low operating voltage (2.5V Max)
- Max operating temperature = 40°C (Case temperature)

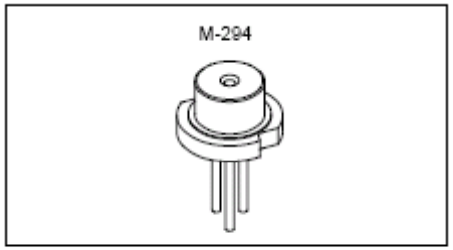

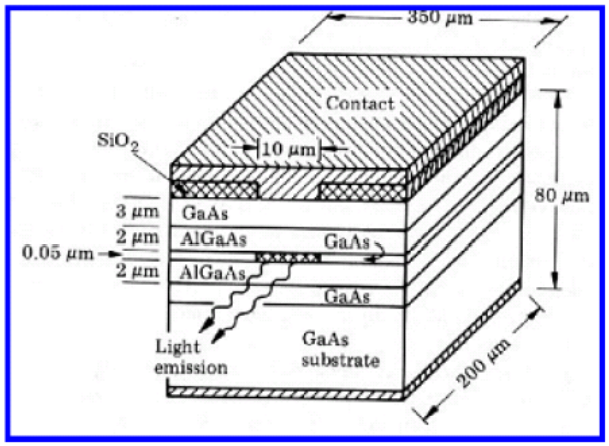

Electrical and Optical Characteristics (Tc = 25°C) Tc: Case temperature

Item		Symbol	Conditions	Min.	Typ.	Max.	Unit
Threshold current		Ith			30	40	mA
Operating current		Iop	Po = 5mW		35	45	mA
Operating voltage		Vop	Po = 5mW		2.2	2.5	V
Wavelength		λp	Po = 5mW		650	660	nm
Radiation angle	Perpendicular	θ⊥	Po = 5mW	22	30	40	degree
	Parallel	θ//		5	7	12	degree
Positional accuracy	Position	ΔX, ΔY, ΔZ	Po = 5mW			±150	μm
	Angle	Δϕ//				±3	degree
		Δϕ⊥				±3	degree
Differential efficiency		ηD	Po = 5mW	0.3	0.6	0.9	mW/mA
Astigmatism		As	Po = 5mW		7	15	μm
Monitor current		Imon	Po = 5mW, VR = 5V	0.05	0.1	0.25	mA

astigmatism

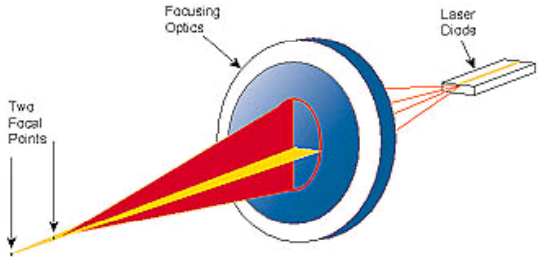

Figure 10. Schematic diagram showing the problem of astigmatism.

Due to the short cavity and the use of an unstable resonator, output beam is highly divergent
Due to the asymmetric cavity geometry, an astigmatic elliptical (anisotropic) beam is obtained
Low coherence (spatial, temporal and, we will see, spectral) achievable!

SPECTRAL PROPERTIES OF A HETEROJUNCTION LASER

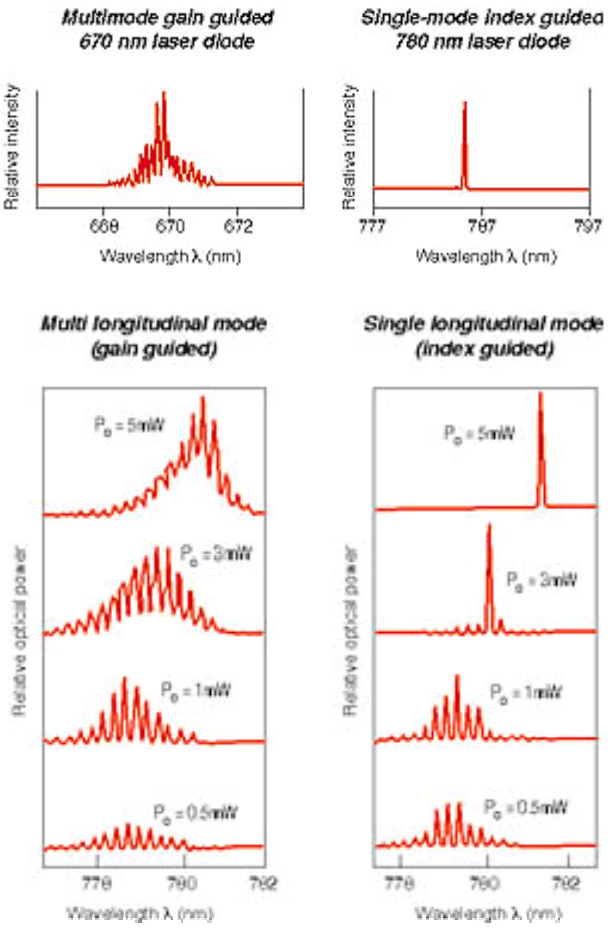

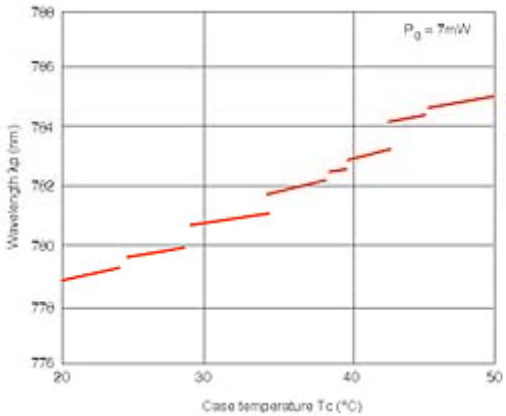

Figure 14. Mode hopping observed while temperature tuning a single-mode laser diode.

Mode jumps at varying *T* → precise temperature stabilization required (at the mK level)!

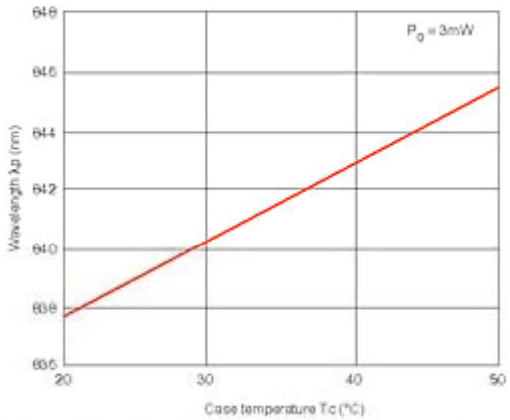

Figure 13. Effects of temperature on center wavelength.

Variation of the caviity length with *T* → The wavelength can be tuned with *T* (~0.2-0.4 nm/K)
Note: tunability in a smaller range (~GHz/mA) can be achieved also by controlling *I* (leading to change the refractive index)

Multimode operation (competition between differenc longitudinal modes) often achieved
Note: $\Delta\nu_{fsr} \sim 10^{11}$ Hz → mode spacing in wavelength units is several Angstrom

GAIN CURVE AND TUNABILITY I

The gain curve of the active medium in a heterojunction laser is typically very broad

This is due to several interconnected reasons:

1. Appearence of bands in the solid state
2. Strong (non radiative) broadening effects
3. MQW and exciton-related effects

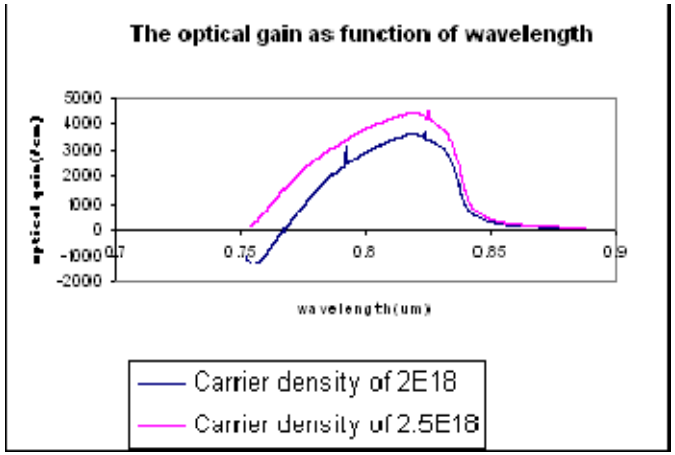

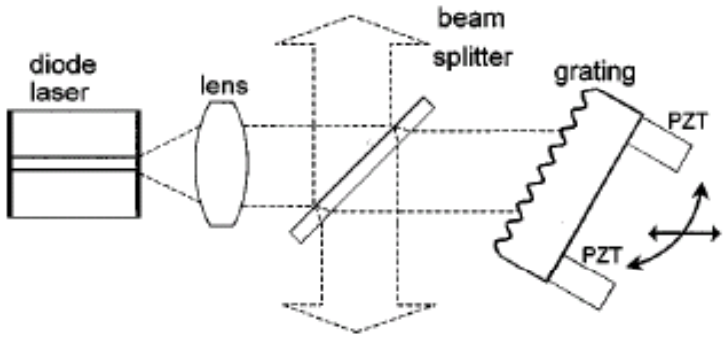

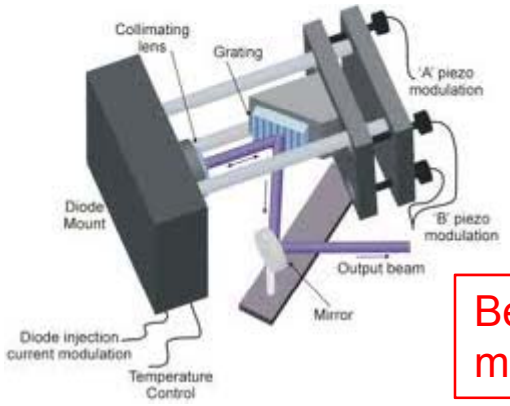

Tunablity (at some extent, typically tens of nm) can be obtained by **coupling with an external cavity** with typical free spectral range of a few GHz

Typically, diffraction grating-ended cavities are used

Note: this is an *external* cavity exploiting the *optical feedback* effect
In fact, due to the poor reflectivity of the end mirrors, the *iternal* cavity of the laser is sensitive to retroreflected beams

Besides tunability, coupling with the external cavity improves monochromaticity (linewidth below the MHz range!)

GAIN CURVE AND TUNABILITY I

External optical cavities can be also integrated (microfabricated) into the laser chip

DFB = Distributed FeedBack Laser - in which the grating is distributed along the entire active medium. The wavelength of the grating determines the wavelength emitted from the laser. This laser emits radiation in a very narrow line spectrum.

DBR = Distributed Bragg Reflector - in which the grating is outside the region of the active medium, in a place where no current flows (the passive part of the cavity).

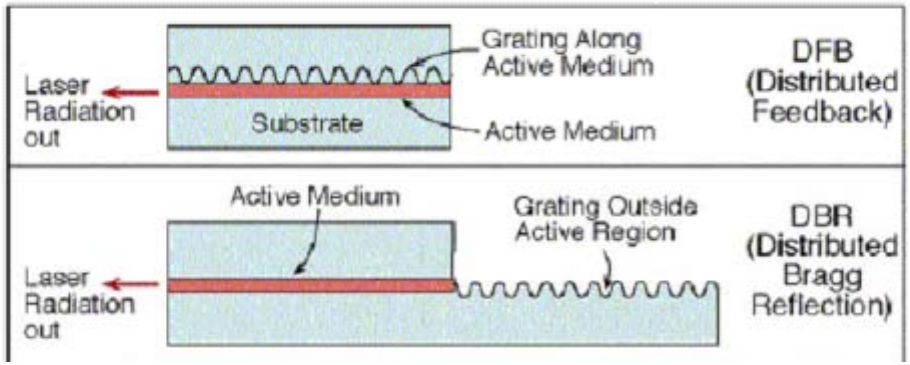

DFB and DBR lasers are available: they show relatively narrow band emission (monochromaticity), typically in the MHz range, and are usually tunable by acting on the temperature (thanks to controlled thermal expansion of the grating)

VERTICAL CAVITY LASER (VCSEL)

Distributed Bragg Reflector structure (*1D photonic crystal)*

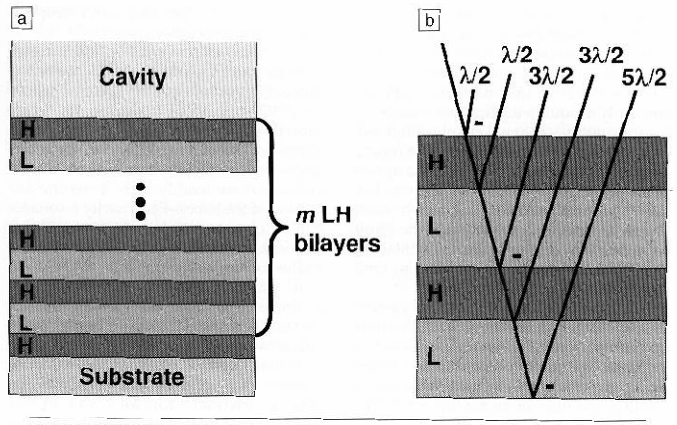

Figure 1. (a) Distributed Bragg reflector (DBR) structure using a high-refractive-index quarter-wave layer on the substrate followed by m low-index/high-index (LH) quarter-wave bilayers. (b) Relative phases at the DBR surface of light rays reflected from each interface within the DBR structure. The minus sign indicates the 180° phase shift that occurs upon reflection from a low- to high-index surface. A round-trip pass through each quarter-wave layer results in a half-wave phase shift. Every reflected ray returns to the DBR surface shifted by exactly 180° in phase. All reflected electric fields thus add constructively to give a high net reflectance for the DBR, even if individual interface reflectances are small.

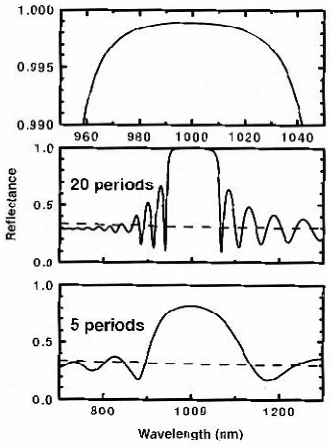

Figure 2. Reflectance spectrum in air of a 1600-nm GaAs/AlAs DBR for 20 periods and 5 periods (lower two plots). Dashed lines show the reflectance from a bare GaAs substrate. Top plot shows the high-reflectance region of the 20-period mirror near the design wavelength.

"Bragg mirrors" can be built by depositing alternate layers with different refractive index and highly controlled thickness

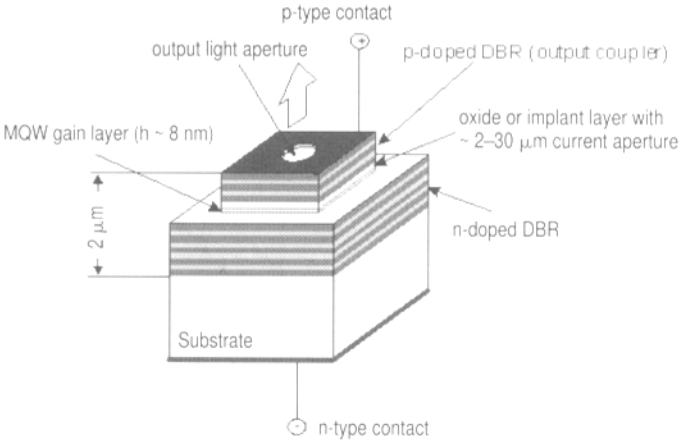

The laser cavity design discussed so far is that of an edge-emitting laser, also known as an in-plane laser, where the laser output emerges from the edge. However, many applications utilizing optical interconnection of systems require a high degree of parallel information throughput where there is a demand for surface emitting laser (SEL). In SEL the laser output is emitted vertically through the surface. Many schematics have been utilized to produce surface emitting lasers. A particularly popular geometry is that of a vertical cavity SEL, abbreviated as VCSEL. This geometry is shown in Figure 4.20. It utilizes an active medium such as multiple quantum wells sandwiched between two distributed Bragg reflectors (DBR), each comprising of a series of material layers of alternating high and low refractive indices. Thus for an InGaAs laser, the DBR typically consists of alternating layers of GaAs with refractive index ~3.5 and AlAs with refractive index 2.9, each layer being a quarter of a wavelength thick. These DBRs act as the two mirrors of a vertical cavity. Thus, both the active layer (InGaAs) and the DBR structures (GaAs, AlAs) can be produced in a continuous growth process.

An advantage offered by a VCSEL is that the lateral dimensions of the laser can be controlled, which offers the advantage that the laser dimensions can be tailored to match the fiber core for fiber coupling. An issue to deal with in VCSEL is the heating effect occurring in a complex multilayer structure, as the current is injected through a high series resistance of the DBRs.

Vertical Cavity Surface Emitting Laser

VCSEL advantages:

- **Surface emission for integration in optoelectronics (e.g., seamless integration with optical fibers)**
- **"short" and engineered cavity: better temperature stability, beam optical features, ...;**
- **Small overall size, low threshold, high efficiency**

PUSHING AHEAD THE FABRICATION PRECISION

QC-laser crystal grown by Molecular Beam Epitaxy (MBE)

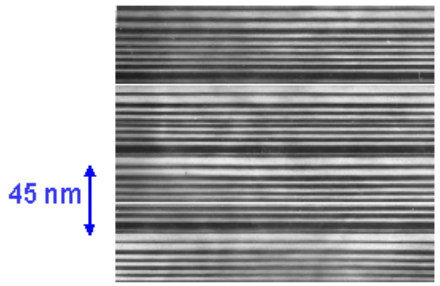

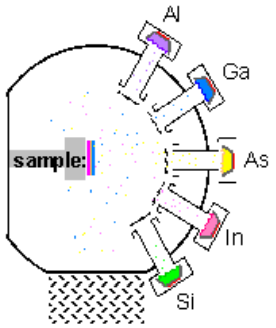

Cross-section of a few stages of QC-laser crystal *crystal growth one atomic layer at a time*

- Many (~ 500), few-atoms thick layers of alloy materials (Al, Ga, As, In);
- atomic control of layer thickness, 1 nanometer (nm) = 4 atomic layers
- atomically flat layer interfaces

Progress in the MBE and related techniques enabled (since the late '90s) highly controlled fabrication of thin multilayered heterostructures with unprecedented precision

MINIBANDS IN MQW WITH MANY LAYERS

A superlattice is formed by a periodic array of quantum structures (quantum wells, quantum wires, and quantum dots). An example of such a superlattice is a multiple quantum well, produced by growth of alternate layers of a wider bandgap (e.g., AlGaAs) and a narrower bandgap (GaAs) semiconductors in the growth (confinement) direction. This type of multiple quantum wells is shown in Figure 4.10a,b by a schematic of their spatial arrangement as well as by a periodic variation of their conduction and valence band edges.

When these quantum wells are widely separated so that the wavefunctions of the electrons and the holes remain confined within individual wells, they can be treated as a set of isolated quantum wells. In this case, the electrons (or the holes) can not tunnel from one well to another. The energies and wavefunctions of electrons (and holes) in each well remain unchanged even in the multiple quantum well arrangement. However, such noninteracting multiple quantum wells (or simply labeled multiple quantum wells) are often utilized to enhance an optical signal (absorption or emission) obtainable from a single well. An example is lasing, to be discussed in the next section, where the stimulated emission is amplified by traversing through multiple quantum wells, each well acting as an independent medium.

To understand the interaction among the quantum wells, one can use a perturbation theory approach similar to treating identical interacting particles with degenerate energy states. As an example, let us take two quantum wells separated by a large distance. At this large separation, each well has a set of quantized levels E_n labeled by quantum numbers $n = 1, 2, \ldots$ along the confinement direction (growth direction). As the two wells are brought close together so that the interaction between them becomes possible, the same energy states E_n of the two wells are no longer degenerate. Two new states E_n^+ and E_n^- result from the symmetric (positive) overlap and antisymmetric (negative) overlap of the wavefunctions of the well. The $E_n^+ = E_n + \Delta_n$ and $E_n^- = E_n - \Delta_n$ are split by twice the interaction parameter Δ_n for level n.

The magnitude of the splitting, $2\Delta_n$, is dependent on the level E_n. It is larger for higher energy levels because the higher the value of n (the higher the energy value E_n), the more the wavefunction extends in the energy barrier region allowing more interaction between the wells.

The case of two wells now can be generalized into the case of N wells. Their interactions lift the energy degeneracy to produce splitting into N levels, which are closely spaced to form a band, the so-called miniband. In an infinite multiple quantum well limit, the width of such a miniband is $4\Delta_n$, where Δ_n is the interaction between two neighboring wells for the level n. This result is shown in Figure 4.11 for the two levels E_1 and E_2 for the case of a superlattice consisting of alternate layers of GaAs (well) and $Al_{0.11}Ga_{0.89}As$ (barrier), each of width 9 nm. For this system, the miniband energies are $E_1 = 26.6$ meV and $E_2 = 87$ meV, with the respective bandwidth of $\Delta E_1 = 2.3$ meV and $\Delta E_2 = 20.2$ meV (Barnham and Vvedensky, 2001). As explained above, the higher-energy miniband (E_2) has a greater bandwidth (ΔE_2) than the lower energy miniband (ΔE_1).

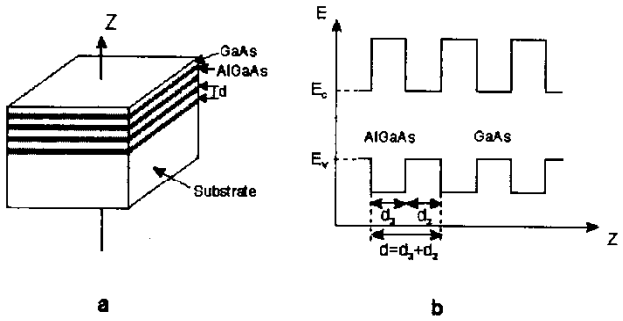

Figure 4.10. Schematics of the arrangement (a) and the energy bands (b) of multiple quantum wells.

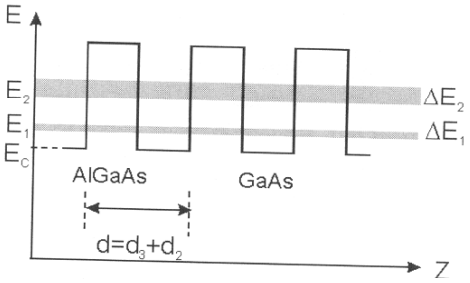

Figure 4.11. Schematics of formation of minibands in a superlattice consisting of alternate layers of GaAs (well) and AlGaAs (barrier).

- ✓ **"Minibands" formed due to interaction of different wells**
- ✓ **This is similar to the formation of bands in crystalline solids due to inter-atom interaction!**

QUANTUM CASCADE LASER (QCL)

Completely new approach to lasing action with the goals:
-Mid-IR lasers with possibility to engineer wavelength (e.g., for trace analysis);
-Huge efficiency (low threshold, high power)

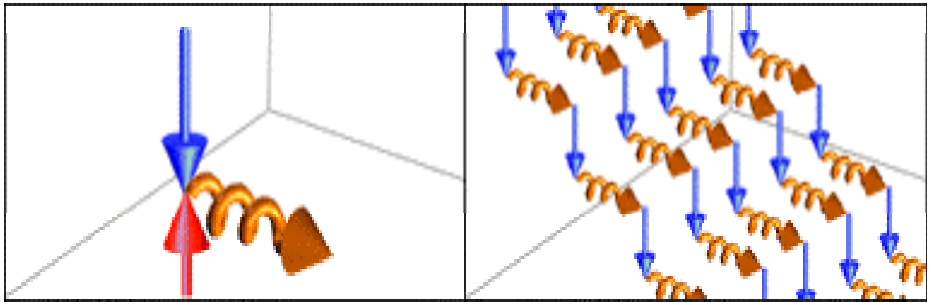

e-h pair recombination is no longer used

Only electrons are involved being the stimulated emission occurring in the intraband (miniband) transitions

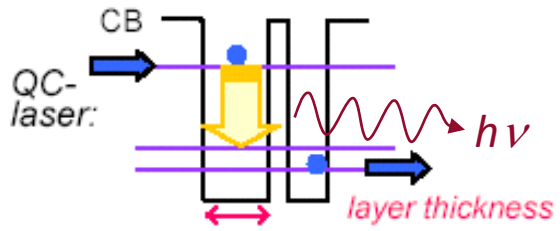

QC-laser:
Light is generated across designed energy ga
"materials by design":
band structure engineering and MBE

- In contrast to the lasers discussed above, which involve the recombination of an electron in the conduction band and a hole in the valence band, the QC lasers use only electrons in the conduction band. Hence they are also called unipolar lasers.
- Unlike the quantum-confined lasers discussed above, which involve an inter-band transition between the conduction band and the valence band, the QC lasers involve intraband (inter-sub-band) transition of electrons between the various sub-bands corresponding to different quantized levels of the conduction band. These sub-bands have been discussed in Section 4.1.
- In the conventional laser design, one electron at the most can emit one photon (quantum yield one). The QC lasers operate like a waterfall, where the electrons cascade down in a series of energy steps, emitting a photon at each step. Thus an electron can produce 25–75 photons.

CASCADE EFFECT

Figure 4.21 illustrates the schematics of the basic design principle of an earlier version of the QC lasers that produce optical output at 4.65 μm. These lasers are based on AlInAs/GaInAs. It consists of electron injectors comprised of a quantum well superlattice in which each quantized level along the confinement is spread into a miniband by the interaction between wells, which have ultrathin (1–3 nm) barrier layers. The active region is where the electron makes a transition from a higher sub-band to a lower sub-band, producing lasing action. The electrons are injected from left to right by the application of an electric field of 70 kV/cm as shown in the slope diagram. Under this field, electrons are injected from the ground state *g* of the miniband of the injector to the upper level 3 of the active region. The thinnest well in the active region next to the injector facilitates electron tunneling from the injector into the upper level in the active region. The laser transition, represented by the wiggly arrow, occurs between levels 3 and 2, because there are more electron populations in level 3 than in level 2. The composition and the thickness of the wells in the active region are judiciously manipulated so that level 2 electron relaxes quickly to level 1.

The cascading process can continue along the direction of growth to produce more photons. In order to prevent accumulation of electrons in level 1, the exit barrier of the active region is, again, made thin, which allows rapid tunneling of electrons into a miniband of the adjacent injector. After relaxing into the ground state *g* of the injector, the electrons are re-injected into the next active region. Each successive active region is at a lower energy than the one before; thus the active regions act as steps in a staircase. Therefore, the active regions and the injectors are engineered to allow the electrons to move efficiently from the top of the staircase to the

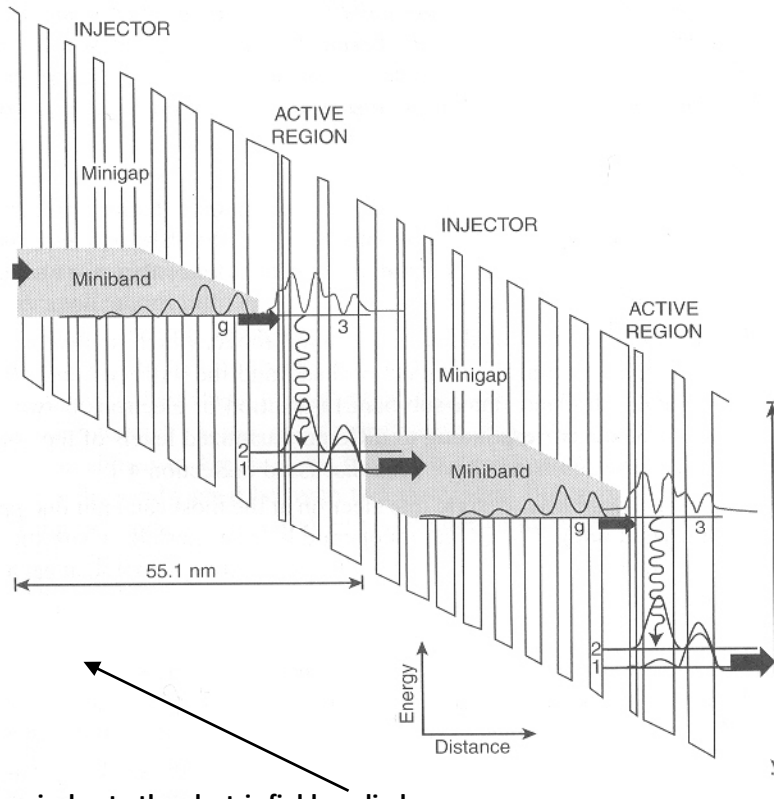

The slope is due to the electric field applied

Careful engineering and manufacturing of electron injector and active layers allow to achieve an efficient cascade behavior →Huge efficiency (each electron produces many photons!)

Tunability can be achieved (at some extent) by playing with the temperature (cavity length) and the electric field strength

KEY FEATURES OF QCLs

Quantum design of QC-laser

J. Faist, F. Capasso, C. Sirtori, D. L. Sivco, J. N. Baillargeon, A. L. Hutchinson, S. N. G. Chu, and A. Y. Cho, Appl. Phys. Lett. ***68****, pp. 3680-3682 (1996).*

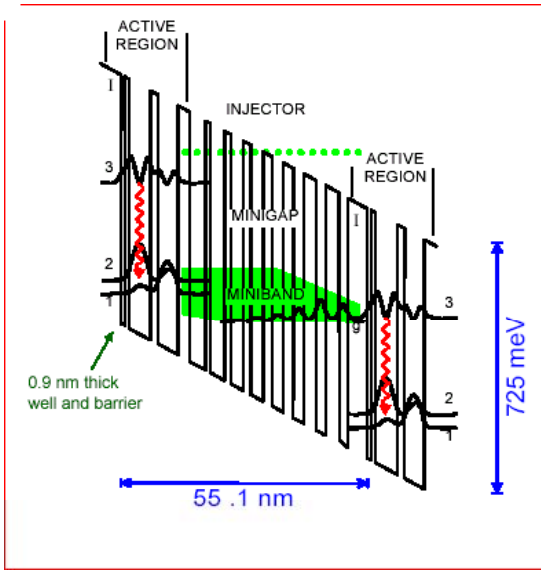

- multiple QWs under external applied electric field
- band-offset = 500 - 800 meV through lattice matched or strain-compensated n InP
- 1 - 100 active regions/injectors (typically ~ 30)
- layer thicknesses designed to provide population inversion $\tau_{32} >> \tau_2$
- designed for tunneling transport

Lucent Technologies
Bell Labs Innovations

Key characteristics of QC-lasers

- Wavelength ("color") determined by layer thickness rather than by material composition

➡ all mid-infrared spectrum covered by the same material

- Each electron creates N laser photons in traversing an N-stage cascaded structure (N = 20 - 75)

➡ intrinsically high power lasers

- High reliability: low failure rate, long lifetime and robust fabrication

Room temperature, pulsed, single-mode QC-DFB laser @ $\lambda \sim 4.65\ \mu m$

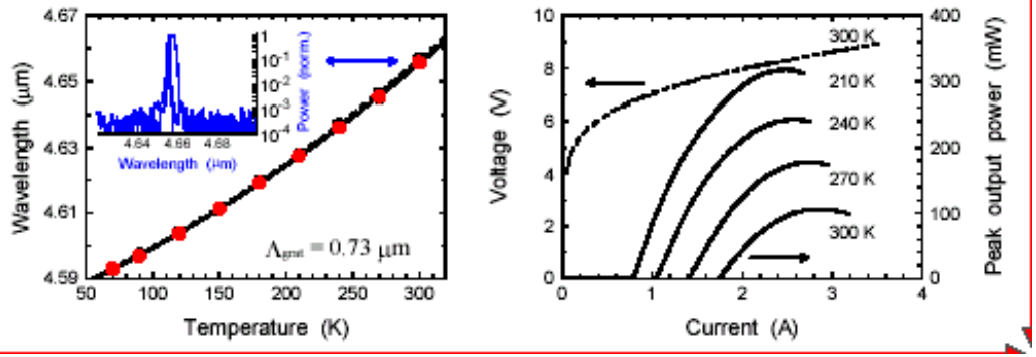

Wide wavelength-range of QC lasers

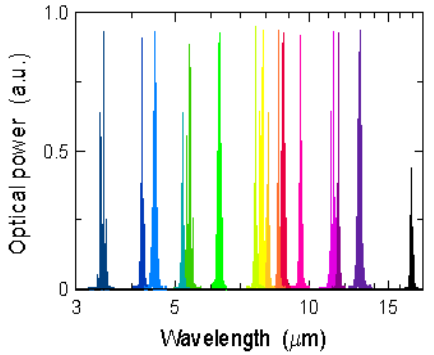

QC lasers cover entire mid-infrared wavelength range (3.4 - 17 μm) by tailoring layer thicknesses of the same material

APPLICATIONS OF QCLs

Remember: molecules and molecular compounds show a large amount of possible transitions associated with vibrations of the molecule itself

Such transitions involv small energy differences → they fall in the infrared range
Such transitions are species selective → they are material fingerprints

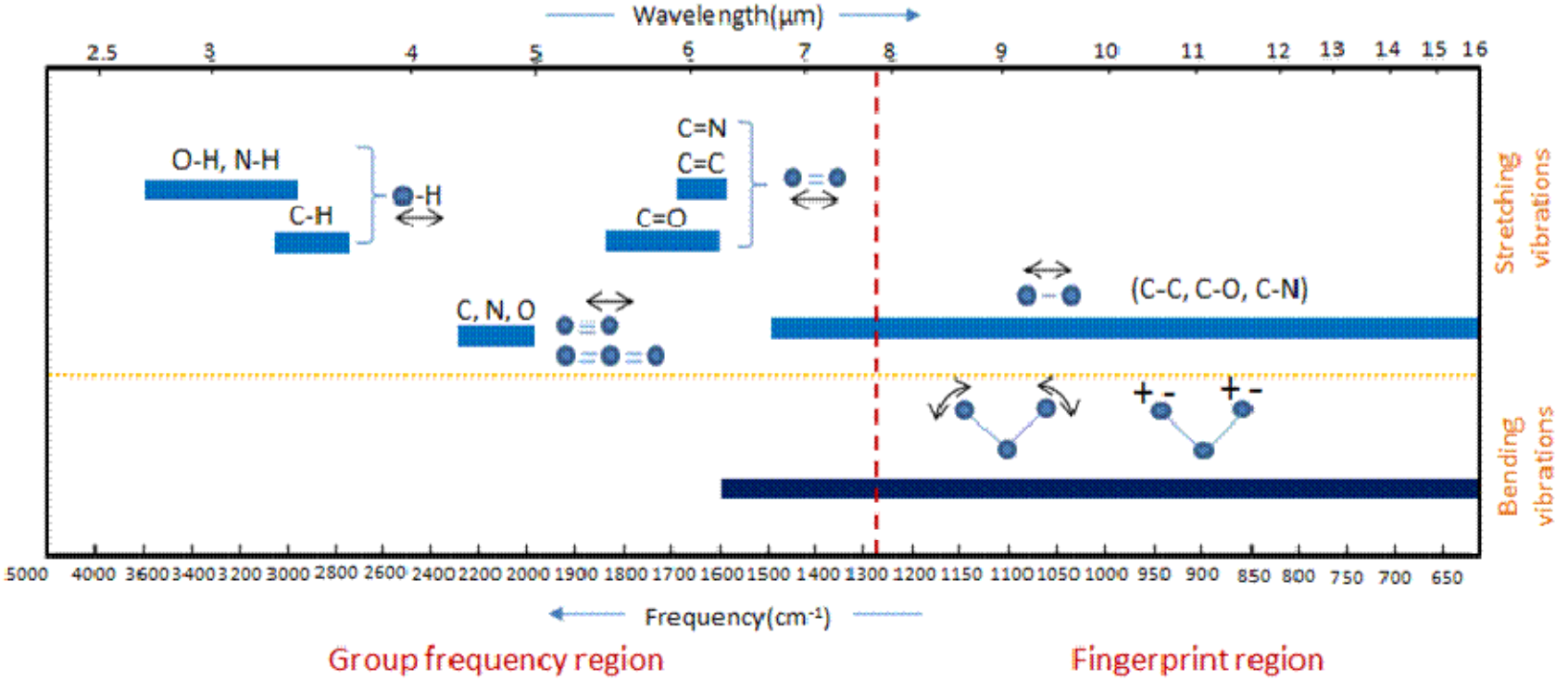

Spectroscopic analysis of molecular fingerprints owns a huge potential for sensing in a variety of fields (materials, pollution, biosensing, etc.)

SPECTROSCOPY OF MOLECULAR FINGERPRINTS

Spectroscopy and the IR fingerprint region

One of the technologies benefiting from the use of these lasers is infrared (IR) spectroscopy. For more than a century, IR spectroscopy has been used to chemically characterize substances by absorption or transmission; more specifically, the spectrum in the 5–14 μm range, part of the so-called "fingerprint region," provides strong and unique (fingerprint-like) characteristics for many substances.

While lasers have long provided dramatic benefits for IR spectroscopy, prior to the invention of QCLs there were no commercially available lasers that could provide light across the fingerprint region in the mid-IR. Fourier transform IR (FTIR) spectrometers have been the standard equipment used for decades to obtain the spectral characteristics of substances, but new QCL-based spectroscopic instruments have significant benefits over these devices.

Quantum-cascade lasers are orders of magnitude brighter than other coherent sources in the fingerprint region, providing enough brightness for standoff, noncontact sensing, and analysis of highly absorbing or scattering targets. The output facets of QCLs are small enough that the light they emit can be imaged to essentially diffraction-limited spots, enabling the analysis of miniature targets at long distances (up to hundreds of meters) and the coupling to small-diameter fibers with very small optical coupling loss.

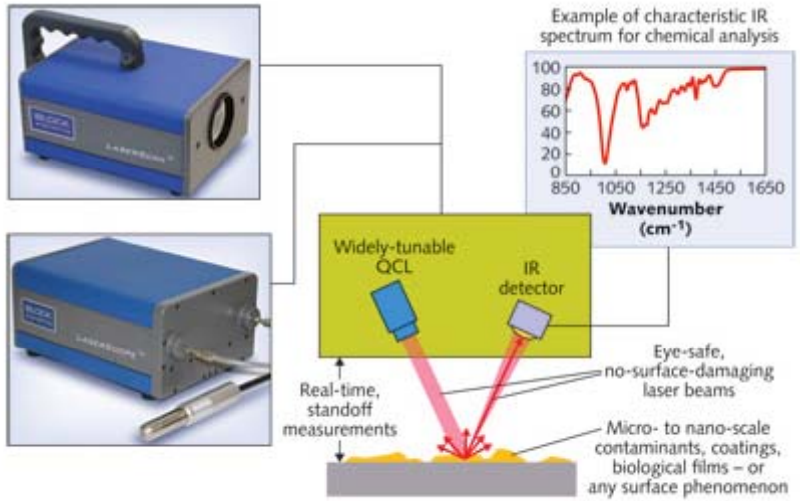

FIGURE 3. In QCL-based surface characterization, a bright, widely tunable laser beam allows standoff measurements using an uncooled IR detector.

QCLs:

- Can made to emit in the desired wavelength range
- Are extremely "brilliant" and rather coherent (the cavity features high-*Q* cavities due to DBR-like mirrors)
- Can be tuned by acting, e.g., on the applied electric field or on the cavity length (thermal expansion)
- Are very powerful and efficient and can lead to remarkably large signal-to-noise ratio
- Are portable, miniaturized and (now) rather unexpensive

Laser Focus – 01/01/2013

CONCLUSIONS

- ✓The evolution and diffusion of diode laser is an interesting case story to study the interplay between fundamental, applicative and technological issues
- ✓Billions of diode lasers have been or are being produced to cope with important large scale applications (e.g., TLC, CD, DVD)
- ✓In spite of its wide diffusion, diode lasers own inherently poor optical properties (enough, however, to distinguish from LEDs!)
- ✓There are technologies able to (partially, at least) overcome conventional limitations
- ✓Among them, QCLs are gaining strong momentum for large scale analytical applications

CREDITS

O. Svelto and P. Hanna, Principles of Lasers (Plenum Press, 1998)
http://www.wikipedia.org
R. Pratesi, *Dispense di Fisica dei Laser*, Università di Firenze ed INO, (http://www.ino.it/home/pratesi/DispenseL&A.htm).
physics today, vari numeri
R. Waser (ed.), *Nanoelectronics and information technology* (Wiley-VCH, 2003)
F. Fuso, Fisica delle Nanotecnologie, trasparenze lezioni 2007/08, e referenze citate
Laura Andreozzi, Laboratorio di Fisica 2
Khanh Kieu http://kald.or.kr
Yu, Cardona, *Fundamentals of Semiconductors* (Springer, 1999)